HHS Public Access
Author manuscript
J Med Chem. Author manuscript; available in PMC 2016 September 24.

Published in final edited form as:
J Med Chem. 2015 September 24; 58(18): 7485–7500. doi:10.1021/acs.jmedchem.5b01005.

Discovery of a Selective and CNS Penetrant Negative Allosteric Modulator of Metabotropic Glutamate Receptor Subtype 3 with Antidepressant and Anxiolytic Activity in Rodents

Julie L. Engers[†], **Alice L. Rodriguez**[†], **Leah C. Konkol**[†,§], **Ryan D. Morrison**[†,‖], **Analisa D. Thompson**[†], **Frank W. Byers**[†], **Anna L. Blobaum**[†], **Sichen Chang**[†], **Daryl F. Venable**[†,⊥], **Matthew T. Loch**[†], **Colleen M. Niswender**[†], **J. Scott Daniels**[†,‖], **Carrie K. Jones**[†], **P. Jeffrey Conn**[†], **Craig W. Lindsley**[†,‡], and **Kyle A. Emmitte**[*,†,‡,#]

[†]Vanderbilt Center for Neuroscience Drug Discovery, Department of Pharmacology, Vanderbilt University Medical Center, Nashville, Tennessee 37232, United States

[‡]Department of Chemistry, Vanderbilt University, Nashville, Tennessee 37232, United States

Abstract

Previous preclinical work has demonstrated the therapeutic potential of antagonists of the group II metabotropic glutamate receptors (mGlus). Still, compounds that are selective for the individual group II mGlus ($mGlu_2$ and $mGlu_3$) have been scarce. There remains a need for such compounds with the balance of properties suitable for convenient use in a wide array of rodent behavioral studies. We describe here the discovery of a selective $mGlu_3$ NAM **106** (VU0650786) suitable for in vivo work. Compound **106** is a member of a series of 5-aryl-6,7-dihydropyrazolo[1,5-*a*]pyrazine-4(5*H*)-one compounds originally identified as a $mGlu_5$ positive allosteric modulator (PAM) chemotype. Its suitability for use in rodent behavioral models has been established by extensive in vivo PK studies, and the behavioral experiments presented here with compound **106** represent the first examples in which an $mGlu_3$ NAM has demonstrated efficacy in models where prior efficacy had previously been noted with nonselective group II antagonists.

[*]**Corresponding Author** Phone: 817-735-0241. Fax: 817-735-2603. kyle.emmitte@unthsc.edu..
[§]**Present Addresses** Incyte Corporation, Experimental Station, E336/131A, Route 141 and Henry Clay Road, Wilmington, Delaware 19880, United States.
[‖]**Present Addresses** Sano Informed Prescribing, Cool Springs Life Sciences Center, 393 Nichol Mill Lane, Suite 34, Franklin, Tennessee 37067, United States.
[⊥]**Present Addresses** Covance Inc., 671 South Meridian Road, Greenfield, Indiana 46140, United States.
[#]**Present Addresses** Department of Pharmaceutical Sciences, UNT System College of Pharmacy, University of North Texas Health Science Center, 3500 Camp Bowie Boulevard, Fort Worth, Texas 76107, United States.

Author Contributions
Drs. Emmitte and Lindsley directed and designed the chemistry. Drs. Engers and Konkol performed the medicinal chemistry. Drs. Conn and Niswender directed and designed the molecular pharmacology experiments. Dr. Rodriguez directed and performed molecular pharmacology experiments. Mr. Venable and Mr. Loch performed molecular pharmacology experiments. Dr. Daniels directed and designed the DMPK experiments. Dr. Blobaum directed DMPK experiments and performed bioanalytical work. Mr. Morrison performed bioanalytical work. Mr. Chang performed in vitro DMPK work. Mr. Byers performed in vivo DMPK work. Dr. Jones directed and designed the behavioral experiments. Dr. Thompson performed the behavioral experiments.

The authors declare no competing financial interest.

Supporting Information
The Supporting Information is available free of charge on the ACS Publications website at DOI: 10.1021/acs.jmedchem.5b01005.
Experimental procedures and spectroscopic data for additional compounds, molecular pharmacology methods, DMPK methods, behavioral pharmacology methods, and the ancillary pharmacology profile details of **106** (PDF)
Molecular formula strings (CSV)

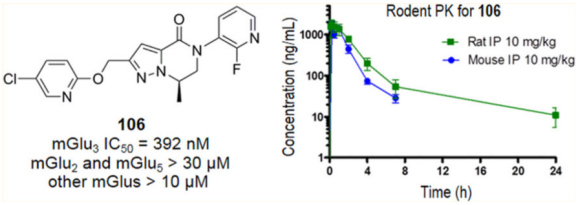

INTRODUCTION

Glutamate (L-glutamic acid) is the major excitatory neuro-transmitter in the mammalian central nervous system (CNS) and acts on both ionotropic and metabotropic glutamate receptors (mGlus). While ionotropic glutamate receptors are ligand-gated ion channels, mGlus are a family of eight G-protein coupled receptors (GPCRs). Belonging to family C of the GPCRs, the mGlus possess a seven transmembrane (7TM) α-helical domain connected via a cysteine-rich region to a large bilobed extracellular amino-terminal domain containing the orthosteric binding site. The mGlus have been further categorized into three groups according to their homology, preferred signal transduction mechanisms, and pharmacology: group I ($mGlu_1$ and $mGlu_5$), group II ($mGlu_2$ and $mGlu_3$), and group III ($mGlu_4$, $mGlu_6$, $mGlu_7$, and $mGlu_8$).[1–3] Both $mGlu_2$ and $mGlu_3$ are primarily located presynaptically in neurons and coupled to $G_{i/o}$ and the inhibition of adenylyl cyclase activity; in addition, $mGlu_3$ is also expressed in glial cells. The group II mGlus are widely expressed throughout the CNS, including regions of the brain associated with emotional states such as the amygdala, hippocampus, and prefrontal cortex.[4,5]

Researchers have been successful in designing both orthosteric antagonists and negative allosteric modulators (NAMs), also known as noncompetitive antagonists, of the group II mGlus. Although such compounds are generally selective versus the other six members of the mGlu family, selectivity between $mGlu_2$ and $mGlu_3$ is negligible.[6] Still, the use of such compounds in animal models has established a potential role for $mGlu_{2/3}$ antagonists in a variety of CNS disorders. Many of these studies have been carried out with two orthosteric antagonists, both of which are highly functionalized glutamate analogues, **1** (LY341495)[7] and **2** (MGS0039)[8] (Figure 1). For example, work with these compounds has helped establish $mGlu_{2/3}$ inhibition as a potential therapeutic application for obsessive-compulsive disorder (OCD),[9,10] anxiety,[11] cognition,[12] and Alzheimer's disease.[13–15] Additionally, antidepressant efficacy has been demonstrated in numerous rodent models of depression with these compounds,[8,9,11,16–19] including those meant to assess treatment-resistant depression (TRD),[20] anhedonia,[21] and depression associated with withdrawal from addictive substances.[22,23] Compound **1** has also been used as a tool to establish a potential utility for $mGlu_{2/3}$ inhibition in the treatment of glioma.[24–27]

Research with $mGlu_{2/3}$ NAMs has been less extensive than with orthosteric antagonists; however, closely related tools **3** (RO4491533)[28] and **4** (RO4432717)[29,30] (Figure 1) have been employed in multiple in vivo assays. In particular, these compounds have demonstrated efficacy in multiple models of depression[31] and cognition.[30,32,33] Furthermore, recent studies in genetically modified mice with **1**[34] and $mGlu_{2/3}$ NAM **6**[35] (Figure 1) point toward a potential application for group II antagonists in the treatment of certain autism spectrum

disorders. Finally, one $mGlu_{2/3}$ NAM, **5** (decoglurant, RO4995819)[36] (Figure 1), has advanced into human clinical trials, including a phase II trial in patients with major depressive disorder (MDD) and resistant to ongoing treatment with antidepressants (NCT01457677).[37] In spite of the wealth of preclinical evidence for the potential utility of $mGlu_{2/3}$ antagonists, identification of compounds with ample selectivity between the two group II mGlus and the balance of pharmacology and drug metabolism and pharmacokinetics (DMPK) properties required for use in vivo has been elusive. Such tools are essential for further validation of the precise roles of each receptor in the etiology of disease.

Our first foray into this arena of research began by an observation of occasional weak $mGlu_3$ NAM activity in a series of 1,2-diphenylethyne $mGlu_5$ positive allosteric modulators (PAMs).[38] An optimization plan for $mGlu_3$ activity that centered on modification of the functional groups appended to the two phenyl rings within this scaffold delivered first-generation tool **7** (VU0463597, ML289)[39] (Figure 2). Importantly, not only was **7** selective versus $mGlu_5$ but selectivity versus $mGlu_2$ was also notable (>15-fold). Further optimization within this chemotype identified a second-generation compound **8** (VU0469942, ML337)[40] (Figure 2) that was devoid of both $mGlu_2$ and $mGlu_5$ activity. While **8** has proven quite useful as an in vitro tool compound and can be used in mice at high doses (100 mg/kg),[41] lower CNS penetration and higher protein binding in rats prevent its utility in that species. Furthermore, 1,2-diarylethyne chemotypes similar to this one are prone to bioactivation at the alkyne moiety and subsequent formation of reactive metabolites that can lead to toxicity.[42,43] Thus, the discovery of a superior $mGlu_3$ NAM from outside the 1,2-diphenylethyne chemotype, with the balance of pharmacology and DMPK properties for convenient use in both rats and mice, remained a worthy goal and is the subject of this manuscript.

RESULTS AND DISCUSSION

Lead Identification

The previous success in identification of an $mGlu_3$ NAM lead with inherently good selectivity versus $mGlu_2$ from a $mGlu_5$ PAM chemotype[39,40] prompted the mining of our internal collection of $mGlu_5$ PAM chemotypes lacking an alkyne moiety. Utilization of this resource provided some examples of compounds with evidence of $mGlu_3$ NAM activity amid the available associated cross-screening data versus the mGlu family.[44,45] We selected many of these interesting compounds as well as additional closely related analogues to arrive at approximately 160 compounds for full concentration response curve (CRC) measurements in our cell-based functional assay for $mGlu_3$. This fluorescence-based assay measures calcium mobilization induced by $mGlu_3$ activation in a cell line stably expressing rat $mGlu_3$ and the promiscuous G-protein $G_{\alpha 15}$ and is capable of detecting agonists, PAMs, and NAMs of $mGlu_3$. We have developed similar assays and cell lines for rat $mGlu_2$ and rat $mGlu_5$, and both were used throughout this project for assessing selectivity.

One of the most interesting series to emerge from the full CRC $mGlu_3$ screen outlined above is exemplified by compounds **9–11** (Figure 3). These compounds are from within a series of 5-aryl-6,7-dihydropyrazolo[1,5-*a*]pyrazine-4(5*H*)-ones that includes many potent $mGlu_5$

PAMs.[46] An interesting piece of SAR was noted with respect to the presence of a chiral methyl group at the seven position of the pyrazine-4(5*H*)-one ring in the (*R*)-configuration (**10**). Whereas the potency of (*R*)-methyl analogue **10** at $mGlu_5$ was only 2-fold less than unsubstituted analogue **9**, the efficacy of **10** (Glu Max = 26.5%) was much weaker than that observed with **9** (Glu Max = 93.0%). The (*S*)-methyl analogue **11** proved highly preferential for $mGlu_5$ PAM activity and was only weakly active at $mGlu_3$, inhibiting the glutamate response only at the top concentration tested (30 μM). Gratifyingly, compound **10** was also inactive up to the top concentration tested (30 μM) in our $mGlu_2$ calcium mobilization assay. Given the potential benefits engendered by this (*R*)-methyl group, we incorporated this functional group into the design of future compounds.

Development of SAR in the Western Region

Our initial plan centered on the development of structure–activity relationships (SAR) in the area occupied by the 2-pyridyl ether of **10**, termed the western region of the scaffold. Intermediate primary alcohol **20** was envisioned as a valuable intermediate for late stage diversification of this area (Scheme 1). The synthesis of **20** began with commercially available phenoxyacetone **12**. The sodium enolate of **12** was prepared and treated in situ with diethyl carbonate to afford 2,4-diketone intermediate **13**. Reaction of **13** with hydrazine readily provided **14**, which could be *N*-alkylated via a Mitsunobu reaction[47] with commercially available chiral alcohol **15**. This Mitsunobu reaction was carried out with microwave heating and resulted in inversion of stereochemistry as expected. Treatment of intermediate **16** with acid resulted in cleavage of the *tert*-butylcarbamate protecting group, and subsequent exposure to aqueous base provided the lactam **17**. Chiral HPLC analysis of **17** showed 98.6% ee for this key intermediate. *N*-Arylation of **17** was accomplished by a copper mediated coupling[48] with 4-fluorobromobenzene to yield **18**. Treatment of **18** with boron tribromide cleaved the phenoxy ether, affording the corresponding primary bromide, which was then reacted with potassium acetate under mild heating to afford acetate ester **19**. Hydrolysis of the acetate group was accomplished with aqueous lithium hydroxide to give the desired intermediate alcohol **20**.

Preliminary $mGlu_3$ NAM SAR obtained from the testing of analogues of lead **10** that were included in the original set of 160 compounds indicated a preference for phenyl and 2-pyridyl ethers in the western portion of the scaffold. Late stage conversion of intermediate alcohol **20** to new analogues was accomplished through one of three methods (Scheme 2). For the synthesis of substituted phenyl ether analogues **22–39**, alcohol **20** was converted to the corresponding mesylate, which was then reacted with the desired phenols **21** and cesium carbonate to afford **22–39**. Alternatively, the phenols **21** and alcohol **20** were coupled directly via a Mitsunobu reaction.[47] For synthesis of 2-pyridyl ether targets **41–51**, the sodium alkoxide of **20** was prepared in situ and treated with substituted 2-fluoropyridines **40** to facilitate a S_NAr reaction and provide **41–51**.

The results obtained from preparing and testing unsubstituted phenyl ether intermediate **18** revealed a near 6-fold preference for $mGlu_5$ vs $mGlu_3$ activity, which ultimately proved a substantial hurdle with this subset of compounds (Table 1). To determine if substitution of the phenyl group could engender preference for $mGlu_3$ activity, we systematically installed a

variety of functional groups at all positions (**22–34**). Most substituents at the 2-position (**22, 26, 29**) only modestly affected $mGlu_3$ NAM activity relative to **18**; however, 2-methoxy analogue **32** was nearly 10-fold less potent than **18**. The $mGlu_5$ PAM activity was improved relative to **18** but remained suboptimal with these 2-substituted analogues. 2,4-Difluoro analogue **25** demonstrated modestly enhanced selectivity versus $mGlu_5$ relative to its monosubstituted comparators **22** and **24**. Although substitution of the 3-position with fluorine (**23**) provided little impact on activity at either receptor, installation of larger substituents (**27, 30, 33**) resulted in reductions in potency at both receptors and two instances of pharmacology mode switching at $mGlu_5$ (**27** and **30**). Such "molecular switches" have been noted previously in other $mGlu_5$ chemotypes.[49,50] Substitution of the 4-position with fluorine (**24**) only minimally impacted potency at either receptor; larger groups (**28, 31, 34**) reduced potency at both receptors, although the effect on $mGlu_5$ was more pronounced. Thus, desiring to further examine the effects of substitution at the 4-position, additional analogues were prepared (**35–39**). The trend toward $mGlu_3$-preferring compounds continued with the 4-ethoxyphenyl analogue **38** and 4-trifluoromethoxy analogue **39**, demonstrating no activity versus $mGlu_5$ up to the highest concentration tested (30 μM).

Given the promising profile of initial lead **10**, our hope for identifying more attractive compounds within the 2-pyridyl analogues (**41–51**) remained high; however, this region proved relatively intolerant of substitution (Table 2). Although a 3-fluoro substituent (**41**) only modestly impacted potency, larger substituents (**42, 43**) had more deleterious effects. Similarly modest results were observed with 4-position (**44–46**) and 6-position (**49–51**) analogues. Still, it was encouraging to identify additional compounds (**42, 43,** and **50**) that displayed no activity versus $mGlu_5$ up to the highest concentration tested (30 μM) as well as several analogues with only weak activity at $mGlu_5$. Fortunately, 5-halo analogues **47** and **48** proved an exception to the general trend of modest $mGlu_3$ potency with these analogues. Furthermore, 5-fluoro analogue **47** demonstrated enhanced selectivity approaching 20-fold versus $mGlu_5$, while 5-chloro analogue **48** was more modest with regard to selectivity at approximately 5-fold.

With some initial SAR in hand, we further profiled some of the more promising early analogues (**38, 47, 48**) to assess other properties important for the development of a useful in vivo tool compound (Table 3). In addition to assessing the degree to which the compounds were bound to rat plasma,[51] the compounds were evaluated in a rat cassette pharmacokinetics (PK) study using intravenous (IV) dosing[52] to assess their metabolic stability in vivo. In spite of its poor selectivity profile versus $mGlu_5$, 4-fluorophenyl ether **24** was also included with these compounds as a comparator compound. In fact, analogue **24** exhibited moderate clearance, with a half-life of over 1.5 h. Not surprisingly, replacement of the fluorine atom (**24**) with the more metabolically labile ethoxy group (**38**) increased clearance to approximately hepatic blood flow and reduced half-life. The results obtained with the 2-pyridyl analogues **47** and **48** revealed a profound metabolic difference. Whereas 5-fluoro analogue **47** was rapidly cleared, 5-chloro analogue **48** had a moderate clearance and a half-life of approximately 2 h. As indicated by their ligand-lipophilicity efficiency (LLE) values,[53] the 2-pyridyl ethers possessed a better balance of potency and lipophilicity than the phenyl ether compounds. Notably, 4-ethoxyphenyl ether **38** also exhibited

exceedingly high protein binding to rat plasma. These factors led to the conclusion that optimization should continue in the context of the 2-pyridyl ethers. Superior LLE, selectivity versus $mGlu_5$, and plasma unbound fraction relative to **48**, made 5-fluoro analogue **47** an attractive starting point for further optimization; however, its high plasma clearance remained an issue. To avoid focusing future optimization efforts exclusively in the context of a potential PK liability, the decision was made to prepare analogues of both **47** and **48** in parallel.

Development of SAR in the Eastern Region

To enable final step diversification and the rapid synthesis of new analogues, modified syntheses were required for development of SAR in the eastern portion of the chemotype. Synthesis of new 5-fluoropyridin-2-yl ether analogues **55–72** was accomplished via a reordering of the previously outlined reactions (Scheme 3). Intermediate **17** was treated with boron tribromide and subsequently potassium acetate to afford acetate ester **52**. Hydrolysis of **52** was accomplished with lithium hydroxide; however, the yield of alcohol **53** suffered due to difficulty in isolation of this polar and water-soluble intermediate. Still, preparation of the 5-fluoropyridin-2-yl ether **54** via S_NAr chemistry was readily accomplished, which enabled a final stage installation of the aryl or heteroaryl eastern ring according to methods described previously to yield the desired products **55–72**.

Because of the poor yield encountered in the synthesis of intermediate **53**, we employed what proved to be a more scalable and shorter synthesis in the preparation of the 5-chloropyridin-2-yl ether analogues (Scheme 4). Synthesis of intermediate **75** from commercially available **73** was accomplished via an analogous two-step Mitsunobu coupling[47] and deprotection/cyclization sequence as described previously. The lactam nitrogen was protected with a 4-methoxybenzyl group to afford **76**. Reduction of the ethyl ester was accomplished with sodium borohydride to yield **77**. Formation of the 5-chloropyridin-2-yl ether **78** was carried out via S_NAr chemistry as before. Oxidative removal of the 4-methoxybenzyl protecting group was carried out with ceric ammonium nitrate to provide penultimate intermediate **79**. Conversion of **79** into analogues **80–110** utilized the copper mediate *N*-arylation methods employed previously.

Testing of new 5-fluoropyridin-2-yl ether analogues **55–72** showed eastern ring modification was a useful strategy for enhancing $mGlu_3$ NAM activity (Table 4). In the case of monosubstituted phenyl ethers (**55–65**), several analogues exhibited $mGlu_3$ IC_{50} values less than 200 nM. Specifically, at the 2-position, fluorine (**55**) and chlorine (**57**) substitution was preferred to methyl (**60**) and methoxy (**63**) substituents, while little difference in $mGlu_3$ activity was observed with variation of the same substituents at the 3-position (**56, 58, 61, 64**). Substitution at the 4-position (**59, 62, 65**) was slightly less favorable. Encouragingly, several of these analogues also demonstrated only weak activity at $mGlu_5$. Some difluorophenyl analogues (**66–68**) were also prepared and found to exhibit good potency. Simple pyridyl analogues (**69–71**) were less potent versus $mGlu_3$ than the majority of the phenyl analogues; however, selectivity versus $mGlu_5$ was notable in the case of **70** and **71**. Finally, simple fluorine substitution of the pyridine ring (**72**) enhanced $mGlu_3$ activity relative to unsubstituted comparator **69**.

Although several of these new 5-fluoropyridin-2-yl ether analogues demonstrated improved $mGlu_3$ NAM potency, modest levels of $mGlu_5$ selectivity, and improved LLE values[53] (Table 5), their DMPK profiles remained a critical unanswered question. Thus, selected analogues were profiled in our aforementioned rat protein binding assay,[51] and metabolic stability was also assessed in vitro by measuring the intrinsic clearance of the compound when incubated with rat liver microsomes (RLM).[54] While the fraction unbound in rat plasma was encouraging for most compounds, metabolic stability was uniformly poor. Unfortunately, on the basis of their intrinsic clearance in RLM, the compounds were predicted to exhibit hepatic clearance near blood flow.[55]

Fortunately, testing of new 5-chloropyridin-2-yl ether analogues **80–101** ultimately provided another path forward for the design of both potent and highly selective $mGlu_3$ NAMs (Table 6). Monosubstituted phenyl analogues (**80–93**) generally exhibited similar activity at $mGlu_3$ (IC_{50} = 200–600 nM) regardless of the position of the substituent on the ring. 4-Chlorophenyl analogue **84**, 2-methoxyphenyl analogue **88**, and 3-cyanophenyl analogue **92** were exceptions to this trend with each exhibiting reduced activity at $mGlu_3$. Although most of these monosubstituted phenyl analogues (**80–93**) demonstrated only modest selectivity versus $mGlu_5$, 4-methylphenyl analogue **87**, 2-methoxyphenyl analogue **88**, and 3-cyanophenyl analogue **92** exhibited weak activity at that receptor. Preparation of disubstituted phenyl analogues (**94–99**) yielded additional compounds with improved selectivity versus $mGlu_5$. 3,5-Difluorophenyl analogue **97** was a weak $mGlu_5$ PAM, and 2-cyano-5-fluorophenyl analogue **98** was inactive versus $mGlu_5$ up to the highest concentration tested (30 μM). Finally, encouraging results were observed with unsubstituted pyridyl analogues **100** and **101**, where both proved inactive versus $mGlu_5$ while maintaining good $mGlu_3$ NAM activity.

Encouraged by the selectivity profiles seen with pyridyl analogues **100** and **101** but suspecting that these unsubstituted compounds may be prone to rapid metabolism, we immediately prepared several substituted analogues of each (Table 7). Unfortunately, in the pyridin-2-yl set (**102–105**), the majority of these modifications enhanced $mGlu_5$ activity, albeit only slightly. Cyano analogue **103** was the lone exception; however, this compound was approximately 2-fold less potent than unsubstituted analogue **100**. Results with the pyridin-3-yl set (**106–110**) were more encouraging as all new compounds except 6-fluoro analogue **110** maintained the excellent selectivity profile versus $mGlu_5$ observed with **101** without a loss of activity at $mGlu_3$. At this point, several compounds with good $mGlu_3$ NAM activity and devoid of $mGlu_5$ activity were in hand, which set the stage for further profiling in pursuit of compounds meriting extensive in vivo evaluation.

As before, we moved several promising compounds into assays to assess protein binding[51] in rat plasma as well as metabolic stability in RLM[54] (Table 8). The lone eastern phenyl analogue **99** was slightly more protein bound than its eastern pyridyl comparators, which was not surprising given its higher lipophilicity. A range of predicted hepatic clearance values based on the intrinsic clearance of the compound in RLM were observed including one analogue of less than one-third hepatic blood flow (**109**) and one analogue near hepatic blood flow (**100**). The remaining analogues were predicted to have moderate clearance in vivo. Somewhat surprisingly, unsubstituted pyridine-3-yl analogue **101** was more

metabolically stable than its regioisomeric comparator **100**. Still, substituted versions of **101** (**106–109**) did exhibit increased stability relative to **101**.

Several interesting analogues were next advanced into rat cassette PK studies using IV dosing[52] to assess their metabolic stability in vivo (Table 9). As the most promising analogue with an eastern phenyl group, **99** was selected for these studies. Unsubstituted eastern pyridyl analogue **101** and several substituted comparators (**106, 108,** and **109**) were also chosen based on the totality of data collected to that point. Distinguishing between analogues **108** and **107** was difficult; however, compound **108** was ultimately selected as it had a marginally better in vitro DMPK profile. 5-Cyanopyridin-3-yl analogue **109** was selected as it was predicted to have the lowest clearance, and 2-fluoropyridin-3-yl analogue **106** was chosen as it was the most potent analogue with a moderate predicted clearance. Compound **99** exhibited a lower clearance in vivo than expected and had a long half-life in excess of 3 h. The in vivo clearance for the pyridine-3-yl analogues was generally well predicted by the RLM experiments, with analogue **108** being the lone exception. Analogues **99, 106,** and **109** were thus selected for further study in single time point (15 min) tissue distribution studies at a higher dose (10 mg/kg).[56] Intraperitoneal (IP) dosing was chosen for these studies as this route is convenient for use in our planned behavioral studies. The same three compounds were also examined in protein binding assays with rat brain homogenates.[51] CNS penetration with each compound was excellent, with compound **106** exhibiting the highest plasma and brain levels. Both **99** and **106** exhibited unbound brain to unbound plasma ratios ($K_{p,uu}$) of one, indicating distribution equilibrium between the compartments and a low probability of the compounds being substrates for transporters.[57] Compound **109** had a $K_{p,uu}$ value of 0.49, indicating possible efflux; however, additional experiments would be required to determine such conclusively. Compound **106** (VU0650786) was deemed the most attractive and targeted for extensive profiling.

Profiling of Compound 106

Profiling of compound **106** began with determination of its full selectivity versus other members of the mGlu family. In addition to $mGlu_5$, selectivity versus fellow group II receptor subtype, $mGlu_2$, was critical to assess. We evaluated the selectivity of **106** versus rat $mGlu_2$ using full CRC analysis, and the compound was inactive up to the highest concentration tested (30 μM). Thus, compound **106** has been established to have no functional activity at either $mGlu_2$ or $mGlu_5$ up to a concentration that is more than 75-fold over the functional potency at $mGlu_3$. The effect of 10 μM **106** on the orthosteric agonist CRC was measured in fold-shift experiments to evaluate selectivity versus the other mGlus.[44,45] No significant effect was found, indicating the compound was inactive at those receptors as well. We further evaluated the nature of the interaction between **106** and $mGlu_3$ by examining the effects of increasing concentrations of **106** on the glutamate CRC in a progressive fold-shift experiment. If an antagonist acts via a noncompetitive mechanism, we anticipate increasing concentrations of antagonist would shift the glutamate curve to the right and decrease the maximal signal of glutamate. Figure 4 depicts the effects of multiple concentrations of **106** and known $mGlu_{2/3}$ NAM **111** (MNI-137)[58] on the glutamate CRC. As expected, both compounds exhibited the characteristic rightward shift and depressed

glutamate maximum typically observed with NAMs, suggesting that **106** does not bind to the orthosteric glutamate binding site but instead acts via an allosteric mechanism.

To evaluate the ancillary pharmacology of the compound, a commercially available radioligand binding assay panel of 68 clinically relevant GPCRs, ion channels, kinases, and transporters was employed,[59] and only a single significant response (5-HT_{2B}, 65% inhibition) was found at 10 μM **106**.[60] Because 5-hydroxytryptamine receptor 2B (5-HT_{2B}) agonists are associated with cardiotoxicity,[61] we followed this result up with a functional cell-based assay to assess potential agonist or antagonist activity of the compound at 5-HT_{2B}.[62] Fortunately, testing up to 10 μM in this assay revealed no functional activity for **106** at 5-HT_{2B}. Potential for drug–drug interactions was negligible as assessed in a human liver microsomes (HLM) cocktail assay with probe substrates for four common P450s (Table 10).[63] Finally, permeability and potential for P-glycoprotein (P-gp) mediated efflux was assessed in Madin–Darby canine kidney (MDCK) cells transfected with the human MDR1 gene.[64] Not surprisingly, compound **106** was highly permeable with no evidence of efflux in this assay.

Confident that **106** possessed a favorable profile with respect to its pharmacology, in vitro DMPK properties, and preliminary in vivo DMPK properties, we moved the compound into several definitive in vivo DMPK studies in rats and mice (Table 11).[56] Time course studies using IP dosing revealed nearly identical and rapidly reached C_{max} values in both rats and mice. A single time point (30 min) tissue distribution study in mice analogous to the one previously conducted in rats showed excellent CNS penetration in that species as well. Again, the $K_{p,uu}$ value was near one as would be expected for a highly permeable compound devoid of efflux issues.[57] A definitive rat IV PK study (1.0 mg/kg) was conducted, and results were essentially identical to those collected with the prior cassette study (0.2 mg/kg). Finally, a rat oral PK study (3.0 mg/kg) was carried out to assess bioavailability, which proved quite good (60%). Taking into account the data summarized herein, it was estimated that the unbound C_{max} in the CNS following the 10 mg/kg IP studies in both rats and mice was at or beyond the measured functional $mGlu_3$ NAM activity. With that in mind, evaluation of compound **106** in rodent behavioral models known to be sensitive to $mGlu_{2/3}$ antagonists was initiated.

Behavioral Pharmacology of Compound 106

It is well-known that naïve mice will bury foreign objects, such as glass marbles, in deep bedding. This behavior can be inhibited by pretreatment with low doses of certain benzodiazepines, such as diazepam,[65] as well as certain selective serotonin reuptake inhibitors (SSRIs), such as fluvoxamine.[66] Likewise, this behavior has proven sensitive to a variety of $mGlu_5$ NAM compounds from diverse chemotypes.[38,67,68] As such, the marble burying assay has often been used as a convenient method for assessing anxiolytic activity. It is worth noting that recent reports have argued that the assay reflects a repetitive and perseverative behavior such as OCD as opposed to novelty-induced anxiety.[69] For our purposes, the most important fact was that the $mGlu_{2/3}$ orthosteric antagonists **1** and **2** have both been previously shown to inhibit marble burying.[9,10] Thus, examination of the selective $mGlu_3$ NAM **106** in this assay was warranted to determine the contribution of $mGlu_2$ versus

$mGlu_3$ to this effect (Figure 5). Gratifyingly, dose dependent efficacy was observed in this assay, with statistically significant effects at all three doses and essentially complete inhibition at the highest dose (56.6 mg/kg). The positive control for this assay was the well characterized $mGlu_5$ NAM 3-[(2-methyl-1,3-thiazol-4-yl)ethynyl]-pyridine (**112**).[70] On the basis of the available DMPK data, it is estimated that CNS unbound exposure of compound **106** at the 10 mg/kg dose in this study reached a peak of 564 nM or approximately 1.5-fold the functional IC_{50}.

Having established its efficacy in an anxiolytic/OCD mouse model, profiling of compound **106** in a rat model of depression was considered valuable for illustrating the utility of the compound. The forced swim test (FST) measures immobility time in rats placed in a tank of water from which they cannot escape and is sensitive to many antidepressants including several SSRIs.[71] Importantly, efficacy with the $mGlu_{2/3}$ orthosteric antagonists **1** and **2** has been demonstrated in this assay,[8] making the examination of **106** compelling (Figure 6). In this case, significant effects in decreasing immobility time were observed at the highest dose (56.6 mg/kg). On the basis of the available DMPK data and an assumption of dose linearity, it is estimated that CNS unbound exposure of **106** at the high dose in these studies reached a peak of 2.3 μM or approximately 6-fold over the functional IC_{50}. The positive control in this assay was the *N*-methyl-D-aspartate (NMDA) receptor antagonist drug ketamine,[72] which was introduced to the market over 50 years ago.[73] Ketamine has recently demonstrated rapid acting antidepressant efficacy in TRD patients.[74–76] Unfortunately, ketamine produces several undesirable side effects including psychotomimetic effects.[77] Preclinical studies implicate common downstream signaling pathways in the antidepressant effects of ketamine and $mGlu_{2/3}$ antagonists, including activation of the α-amino-3-hydroxy-5-methyl-4-isoxazolepropionic acid (AMPA) receptor and the mammalian target of rapamycin (mTOR) pathway.[18,19,78–82] Such studies have raised the possibility that $mGlu_{2/3}$ antagonists or selective antagonists of each individual group II mGlu might represent novel approaches to rapid acting antidepressants without the side effect profile of ketamine. A selective and CNS penetrant $mGlu_3$ NAM compound such as **106** will be a valuable tool in shedding light on such questions.

CONCLUSION

A cross screening hit from a nonalkyne $mGlu_5$ PAM chemotype served as a successful launching point for the discovery of compound **106**, a highly selective $mGlu_3$ NAM with DMPK properties that enable its convenient use in rodent models of psychiatric disorders. In addition to these features, the compound displays moderate clearance and good bioavailability in rats. Furthermore, the compound is highly permeable, not a substrate for P-gp mediated efflux, and possesses an attractive P450-inhibition profile. The compound has demonstrated efficacy in two rodent models previously shown to be sensitive to $mGlu_{2/3}$ inhibition. This highly selective $mGlu_3$ NAM can thus serve as a useful tool for elucidating the role of selective inhibition of $mGlu_3$ and its potential utility as a novel therapeutic target. Such studies will constitute the subject of future communications.

EXPERIMENTAL SECTION

Diethyl (*R*)-1-(1-((*tert*-Butoxycarbonyl)amino)propan-2-yl)-1*H*-pyrazole-3,5-dicarboxylate (74)

Diethyl 3,5-pyrazoledicarboxylate **73** (4.24 g, 20 mmol, 1.0 equiv) and *tert*-butyl (*S*)-(2-hydroxypropyl) carbamate **15** (7.01 g, 40 mmol, 2.0 equiv) were dissolved in THF (100 mL. 0.2 M), and triphenyl phosphine (9.44 g, 36 mmol, 1.8 equiv) was added. After 5 min, the mixture was cooled to 0 °C and di-*tert*-butyl azodicarboxylate (8.29 g, 36 mmol, 1.8 equiv) was added. The reaction mixture was then subjected to microwave irradiation for 25 min at 120 °C. The mixture was cooled to room temperature, and the solvent was removed in vacuo. Purification via flash chromatography on silica gel provided the title compound as a semisolid (8.2 g, yield was not determined due to contamination of D^{t}BAD byproduct, di-*tert*-butyl hydrazine-1,2-dicarboxylate). ^{1}H NMR (400 MHz, MeOD) δ 7.29 (s, 1H), 5.69–5.01 (m, 1H), 4.41–4.35 (m, 4H), 3.51–3.39 (m, 2H), 1.51 (d, J = 6.8 Hz, 3H), 1.41–1.38 (m, 15H). ^{13}C NMR (100 MHz, $CDCl_3$) δ 161.7, 159.0, 155.8, 142.6, 134.2, 114.0, 79.4, 61.4, 61.1, 53.4, 45.1, 28.2 (3C), 18.5, 14.3, 14.2. LCMS (method A): R_T = 1.052 min, *m/z* = 314.2 [M + H]$^+$. HRMS, calcd for $C_{17}H_{27}N_3O_6$ [M], 369.1900; found, 369.1899.

Ethyl (*R*)-7-Methyl-4-oxo-4,5,6,7-tetrahydropyrazolo[1,5-*a*]-pyrazine-2-carboxylate (75)

Compound **74** (8.2 g, 22.2 mmol, 1.0 equiv) was treated with a solution of 4 N HCl in 1,4-dioxane (78 mL). Deprotection of the *tert*-butyl carbamate protecting group was monitored by LCMS. Once deprotection was complete, the reaction mixture was carefully basified with saturated aqueous $NaHCO_3$ (verified by pH paper) and was allowed to stir at room temperature overnight. The mixture was diluted with dichloromethane, and the aqueous layer was extracted with dichloromethane (3×). The combined organic layers were washed with brine, dried over Na_2SO_4, and concentrated in vacuo to provide the title compound as a white solid (4.4 g, 89% yield over two steps), which was used without further purification. ^{1}H NMR (400 MHz, $CDCl_3$) δ 7.35 (s, 1H), 7.13 (bs, 1H), 4.68–4.62 (m, 1H), 4.41 (q, J = 7.1 Hz, 2H), 3.86 (ddd, J = 15.8, 10.2, 1.4 Hz, 1H), 3.51 (ddd, J = 9.4, 6.4, 3.0 Hz, 1H), 1.65 (d, J = 6.6 Hz, 3H), 1.39 (t, J = 7.1 Hz, 3H). ^{13}C NMR (100 MHz, $CDCl_3$) δ 161.7, 159.3, 143.8, 134.4, 110.7, 61.3, 53.2, 46.0, 17.4, 14.3. LCMS (method A): R_T = 0.546 min, *m/z* = 224.2 [M + H]. HRMS, calcd for $C_{10}H_{13}N_3O_3$ [M], 223.0957; found, 223.0957. $[\alpha]^{25}_D$ = −29.9° (c 0.500, $CHCl_3$).

Ethyl (*R*)-5-(4-Methoxybenzyl)-7-methyl-4-oxo-4,5,6,7-tetrahydropyrazolo[1,5-*a*]pyrazine-2-carboxylate (76)

Compound **75** (2.23 g, 10 mmol, 1.0 equiv) was dissolved in DMF (50 mL, 0.2 M), cooled to 0 °C, and treated with 60% sodium hydride in mineral oil (480 mg, 12 mmol, 1.2 equiv) in five portions. The reaction mixture was stirred for 15 min, and 4-methoxybenzyl chloride (1.63 mL, 12 mmol, 1.2 equiv) was added. After 16 h, the reaction mixture was diluted with water and extracted with EtOAc (3×). The combined extracts were washed with water and brine, dried over Na_2SO_4, filtered, and concentrated in vacuo. The crude material was purified by flash chromatography on silica gel to provide the title compound (2.51 g, 73% yield) as a pale-yellow solid. ^{1}H NMR (400 MHz, $CDCl_3$) δ 7.37 (s, 1H), 7.23 (d, J = 14.1, 2H), 6.87 (d, J = 14.1, 2H), 4.76 (d, J = 14.5, 1H), 4.59–4.50 (m, 2H), 4.44–4.36 (m, 2H),

3.79 (s, 3H), 3.69 (dd, J = 13.1, 4.6 Hz, 1H), 3.35 (dd, J = 13.1, 6.3 Hz, 1H), 1.47 (d, J = 6.6 Hz, 3H), 1.38 (t, J = 7.0 Hz, 3H). ^{13}C NMR (100 MHz, $CDCl_3$) δ 161.7, 159.5, 137.1, 143.9, 134.8, 129.9 (2C), 127.9, 114.3, 110.9 (2C), 61.2, 55.3, 52.9, 50.4, 48.8, 17.5, 14.3. LCMS (method A): R_T = 0.955 min, m/z = 344.2 [M + H]$^+$. HRMS, calcd for $C_{18}H_{21}N_3O_4$ [M], 343.1532; found, 343.1533. $[\alpha]^{25}_D$ = −8.1° (c 0.157, $CHCl_3$).

(*R*)-2-(Hydroxymethyl)-5-(4-methoxybenzyl)-7-methyl-6,7-dihydropyrazolo[1,5-*a*]pyrazin-4(5*H*)-one (77)

Sodium borohydride (1.16 g, 30.6 mmol, 5.0 equiv) was added slowly to a solution of compound **76** (2.1 g, 6.11 mmol, 1.0 equiv) in THF (20 mL) and MeOH (5.0 mL) at 0 °C. The reaction was heated to 60 °C, and after 30 min at that temperature, the reaction mixture was diluted with water and extracted with dichloromethane. The aqueous layer was acidified with a 1 M aqueous HCl solution and extracted with dichloromethane (2×). The combined extracts were dried over Na_2SO_4 and concentrated in vacuo. Purification by flash chromatography on silica gel provided the title compound as a viscous oil (1.55 g, 84% yield). ^{1}H NMR (400 MHz, $CDCl_3$) δ 7.23–7.21 (m, 2H), 6.87–6.84 (m, 3H), 4.72 (d, J = 14.5 Hz, 1H), 4.68 (s, 2H), 4.59 (d, J = 14.4 Hz, 1H), 4.43–4.35 (m, 1H), 3.78 (s, 3H), 3.60 (dd, J = 13.0, 4.6 Hz, 1H), 3.31 (dd, J = 13.0, 7.4 Hz, 1H), 1.42 (d, J = 6.5 Hz, 3H). ^{13}C NMR (100 MHz, $CDCl_3$) δ 159.4, 157.8, 152.6, 134.5, 129.8 (2C), 128.2, 114.3 (2C), 106.5, 58.7, 55.3, 52.0, 50.8, 48.7, 17.2. LCMS (method A): R_T = 0.680 min, m/z = 302.2 [M + H]$^+$. HRMS, calcd for $C_{16}H_{19}N_3O_3$ [M], 301.1426; found, 301.1428. $[\alpha]^{25}_D$ = −5.3° (c 0.98, $CHCl_3$).

(*R*)-2-(((5-Chloropyridin-2-yl)oxy)methyl)-5-(4-methoxybenzyl)-7-methyl-6,7-dihydropyrazolo[1,5-*a*]pyrazin-4(5*H*)-one(78)

To a solution of compound 77 (1.5 g, 4.98 mmol, 1.0 equiv) in DMF (25 mL, 0.2 M) at 0 °C was added NaH (300 mg, 12.44 mmol, 2.5 equiv). The resulting mixture was stirred for 15 min, and 5-chloro-2-fluoropyridine (1.25 mL, 12.44 mmol, 2.5 equiv) was added. The mixture was stirred overnight and extracted with EtOAc (3×). The combined extracts were concentrated in vacuo. Purification by flash chromatography on silica gel afforded the title compound (1.72 g, 84% yield) as a viscous oil. ^{1}H NMR (400 MHz, $CDCl_3$) δ 8.13 (d, J = 2.6 Hz, 1H), 7.54 (dd, J = 8.8, 2.6 Hz, 1H), 7.25 (d, J = 8.5 Hz, 2H), 6.98 (s, 1H), 6.88 (d, J = 8.5 Hz, 2H), 6.75 (d, J = 8.8 Hz, 1H), 5.39 (s, 2H), 4.75 (d, J = 14.5 Hz, 1H), 4.63 (d, J = 14.5 Hz, 1H), 4.50–4.42 (m, 1H), 3.81 (s, 3H), 3.64 (dd, J = 13.0, 4.6 Hz, 1H), 3.35 (dd, J = 13.0, 7.4 Hz, 1H), 1.48 (d, J = 6.5 Hz, 3H). ^{13}C NMR (100 MHz, $CDCl_3$) δ 161.6, 159.4, 157.7, 148.9, 145.1, 138.6, 134.5, 129.8 (2C), 128.2, 124.4, 114.2 (2C), 112.3, 108.2, 61.6, 55.3, 52.1, 50.8, 48.8, 17.2. LCMS (method A): R_T = 1.080 min, m/z = 413.2 [M + H]$^+$. HRMS, calcd for $C_{21}H_{21}ClN_4O_3$ [M], 412.1302; found, 412.1305. $[\alpha]^{25}_D$ = −10.3° (c 1.512, $CHCl_3$).

(*R*)-2-(((5-Chloropyridin-2-yl)oxy)methyl)-7-methyl-6,7-dihydropyrazolo[1,5-*a*]pyrazin-4(5*H*)-one (79)

Compound **78** (1.65 mg, 4.0 mmol, 1.0 equiv) was dissolved in MeCN (40 mL, 0.1 M). and a solution of ceric ammonium nitrate (6.57 g, 12 mmol, 4.0 equiv) in water (12 mL) was

added. After 30 min at room temperature, solvents were removed in vacuo. Purification using flash chromatography on silica gel provided the title compound (764 mg, 65% yield) as a pale-yellow solid. ^{1}H NMR (400 MHz, DMSO-d_6) δ 8.26 (d, J = 2.7 Hz, 1H), 8.21 (s, 1H), 7.83 (dd, J = 8.8, 2.7 Hz, 1H), 6.92 (dd, J = 8.8, 0.5 Hz, 1H), 6.77 (s, 1H), 5.29 (s, 2H), 4.51–4.46 (m, 1H), 3.66 (ddd, J = 13.0, 8.7, 8.7 Hz, 1H), 3.34 (ddd, J = 13.1, 7.9, 2.2 Hz, 1H), 1.45 (d, J = 6.5 Hz, 3H). ^{13}C NMR (100 MHz, DMSO-d_6) δ 161.9, 158.7, 147.7, 145.3, 139.7, 135.1, 124.1, 112.9, 107.4, 61.7, 52.3, 45.6, 17.0. LCMS (method A): R_T = 0.804 min, m/z = 293.2 [M + H]$^+$. HRMS, calcd for $C_{13}H_{13}ClN_4O_2$ [M], 292.0727; found, 292.0727. $[\alpha]^{25}_D$ = −38.3° (c 0.442, $CHCl_3$).

(*R*)-2-(((5-Chloropyridin-2-yl)oxy)methyl)-5-(2-fluoropyridin-3-yl)-7-methyl-6,7-dihydropyrazolo[1,5-*a*]pyrazin-4(5*H*)-one(106)

Copper(I) iodide (13.7 mg, 0.072 mmol, 2.1 equiv) was added to a suspension of compound **79** (10 mg, 0.035 mmol, 1.0 equiv), 3-bromo-2-fluoropyridine (7.40 μL, 0.072 mmol, 2.1 equiv), potassium carbonate (10 mg, 0.072 mmol, 2.1 equiv), and *N*,*N*′-dimethylethylenediamine (20.7 μL, 0.19 mmol, 5.5 equiv) in toluene (0.44 mL) in a sealed reaction vial. The reaction mixture was stirred at 120 °C. After 16 h, the mixture was diluted with EtOAc, filtered through a Celite pad which was rinsed with EtOAc (2×), and concentrated in vacuo. Purification using reserve phase HPLC method 1 with 39–71% CH_3CN in H_2O (0.1% TFA) over 4 min provided the title compound (7.2 mg, 53% yield) as a white powder. ^{1}H NMR (400 MHz, DMSO-d_6) δ 8.27 (dd, J = 2.7, 0.5 Hz, 1H), 8.23 (ddd, J = 4.8, 2.7, 2.7 Hz, 1H), 8.09 (ddd, J = 9.6, 7.7, 1.8 Hz, 1H), 7.84 (dd, J = 8.8, 2.7 Hz, 1H), 7.50 (ddd, J = 9.0, 4.9, 1.3 Hz, 1H) 6.95 (s, 1H), 6.92 (d, J = 0.5 Hz, 1H), 5.35 (s, 2H), 4.82–4.75 (m, 1H), 4.27 (dd, J = 12.8, 4.3 Hz, 1H), 3.98 (dd, J = 12.8, 7.2 Hz, 1H) 1.55 (d, J = 6.5 Hz, 3H). ^{13}C NMR (100 MHz, DMSO-d_6) δ 161.9, 158.2 (d, $J_{C,F}$ = 239 Hz), 156.6, 148.4, 146.4 (d, $J_{C,F}$ = 14 Hz), 145.3, 133.9 (d, $J_{C,F}$ = 13 Hz), 139.8, 134.0, 124.4 (d, $J_{C,F}$ = 28 Hz), 124.2, 123.2 (d, $J_{C,F}$ = 4 Hz), 112.9, 108.7, 61.6, 54.0, 52.7, 17.1. LCMS (method A): R_T = 0.944 min, m/z = 388.2 [M + H]$^+$. HRMS, calcd for $C_{18}H_{15}ClFN_5O_2$ [M], 387.0898; found, 387.0899. $[\alpha]^{25}_D$ = −23.6° (c 0.100, DMSO).

Supplementary Material

Refer to Web version on PubMed Central for supplementary material.

ACKNOWLEDGMENTS

We gratefully acknowledge the generous support of the National Institute of Mental Health for the funding of this work, NIMH R01MH099269 (K.A.E) and U54MH084659 (C.W.L.).

ABBREVIATIONS USED

Ac	acetate
AMPA	α-amino-3-hydroxy-5-methyl-4-isoxazolepropionic acid
AUC	area under the curve
C	concentration

CL	clearance
CNS	central nervous system
CRC	concentration response curve
DIAD	di-*iso*-propyl azodicarboxylate
DMF	*N*,*N*-dimethylformamide
DMPK	drug metabolism and pharmacokinetics
DMSO	dimethyl sulfoxide
D^{t}BAD	di-*tert*-butyl azodicarboxylate
Et	ethyl
FST	forced swim test
F	bioavailability
F_u	fraction unbound
GPCR	G-protein-coupled receptors
HLM	human liver microsomes
IP	intraperitoneal
IV	intravenous
K_p	brain to plasma ratio
$K_{p,uu}$	unbound brain to unbound plasma ratio
LLE	ligand-lipophilicity efficiency
max	maximum
MDCK	Madin–Darby canine kidney
MDD	major depressive disorder
Me	methyl
mGlu	metabotropic glutamate receptor
Ms	methanesulfonyl
mTOR	mammalian target of rapamycin
NAM	negative allosteric modulator
NMDA	*N*-methyl-D-aspartate
OCD	obsessive-compulsive disorder
PAM	positive allosteric modulator
PEG	polyethylene glycol
Ph	phenyl

PK	pharmacokinetics
PO	oral
PS	polystyrene
RLM	rat liver microsomes
SAR	structure–activity relationships
THF	tetrahydrofuran
TRD	treatment-resistant depression
T	time
$t_{1/2}$	half-life
V_{SS}	volume of distribution at steady-state
5-HT$_{2B}$	5-hydroxytryptamine receptor 2B
7TM	seven transmembrane

REFERENCES

1. Niswender CM, Conn PJ. Metabotropic glutamate receptors: Physiology, pharmacology, and disease. Annu. Rev. Pharmacol. Toxicol. 2010; 50:295–322. [PubMed: 20055706]
2. Schoepp DD, Jane DE, Monn JA. Pharmacological agents acting at subtypes of metabotropic glutamate receptors. Neuro-pharmacology. 1999; 38:1431–1476.
3. Conn PJ, Pin J-P. Pharmacology and functions of metabotropic glutamate receptors. Annu. Rev. Pharmacol. Toxicol. 1997; 37:205–237. [PubMed: 9131252]
4. Chaki S, Ago Y, Palucha-Paniewiera A, Matrisciano F, Pilc A. mGlu2/3 and mGlu5 receptors: Potential targets for novel antidepressants. Neuropharmacology. 2013; 66:40–52. [PubMed: 22640631]
5. Palucha A, Pilc A. Metabotropic glutamate receptor ligands as possible anxiolytic and antidepressant drugs. Pharmacol. Ther. 2007; 115:116–147. [PubMed: 17582504]
6. Célanire S, Sebhat I, Wichmann J, Mayer S, Schann S, Gatti S. Novel metabotropic glutamate receptor 2/3 antagonists and their therapeutic applications: a patent review (2005 − present). Expert Opin. Ther. Patents. 2015; 25:69–90.
7. Ornstein PL, Bleisch TJ, Arnold MB, Kennedy JH, Wright RA, Johnson BG, Tizzano JP, Helton DR, Kallman MJ, Schoepp DD, Hérin M. 2-Substituted (2*SR*)-2-amino-2-((1*SR*,2*SR*)-2-carboxycycloprop-1-yl)glycines as potent and selective antagonists of group II metabotropic glutamate receptors. 2. Effects of aromatic substitution, pharmacological characterization, and bioavailability. J. Med. Chem. 1998; 41:358–378. [PubMed: 9464367]
8. Chaki S, Yoshikawa R, Hirota S, Shimazaki T, Maeda M, Kawashima N, Yoshimizu T, Yasuhara A, Sakagami K, Okuyama S, Nakanishi S, Nakazato A. MGS0039: a potent and selective group II metabotropic glutamate receptor antagonist with antidepressant-like activity. Neuropharmacology. 2004; 46:457–467. [PubMed: 14975669]
9. Bespalov AY, van Gaalen MM, Sukhotina IA, Wicke K, Mezler M, Schoemaker H, Gross G. Behavioral characterization of the mGlu group II/III receptor antagonist, LY-341495, in animal models of anxiety and depression. Eur. J. Pharmacol. 2008; 592:96–102. [PubMed: 18634781]
10. Shimazaki T, Iijima M, Chaki S. Anxiolytic-like activity of MGS0039, a potent group II metabotropic glutamate receptor antagonist, in a marble-burying behavior test. Eur. J. Pharmacol. 2004; 501:121–125. [PubMed: 15464070]

11. Yoshimizu T, Shimazaki T, Ito A, Chaki S. An mGluR2/3 antagonist, MGS0039, exerts antidepressant and anxiolytic effects in behavioral models in rats. Psychopharmacology. 2006; 186:587–593. [PubMed: 16612616]
12. Higgins GA, Ballard TM, Kew JN, Richards JG, Kemp JA, Adam G, Woltering T, Nakanishi S, Mutel V. Pharmacological manipulation of mGlu2 receptors influences cognitive performance in the rodent. Neuropharmacology. 2004; 46:907–917. [PubMed: 15081787]
13. Kim SH, Steele JW, Lee SW, Clemenson GD, Carter TA, Treuner K, Gadient R, Wedel P, Glabe C, Barlow C, Ehrlich ME, Gage FH, Gandy S. Proneurogenic group II mGluR antagonist improves learning and reduces anxiety in Alzheimer Aβ oligomer mouse. Mol. Psychiatry. 2014; 19:1235–1242. [PubMed: 25113378]
14. Kim SH, Fraser PE, Westaway D, St. George-Hyslop PH, Ehrlich ME, Gandy S. Group II metabotropic glutamate receptor stimulation triggers production and release of Alzheimer's amyloid β_{42} from isolated intact nerve terminals. J. Neurosci. 2010; 30:3870–3875. [PubMed: 20237257]
15. Yoshimizu T, Chaki S. Increased cell proliferation in the adult mouse hippocampus following chronic administration of group II metabotropic glutamate receptor antagonist, MGS0039. Biochem. Biophys. Res. Commun. 2004; 315:493–496. [PubMed: 14766235]
16. Gleason SD, Li X, Smith IA, Ephlin JD, Wang XS, Heinz BA, Carter JH, Baez M, Yu J, Bender DM, Witkin JM. mGlu2/3 agonist-induced hyperthermia: An in vivo assay for detection of mGlu2/3 receptor antagonism and its relation to antidepressant-like efficacy in mice. CNS Neurol. Disord.: Drug Targets. 2013; 12:554–566. [PubMed: 23574174]
17. Koike H, Fukumoto K, Iijima M, Chaki S. Role of BDNF/TrkB signaling in antidepressant-like effects of a group II metabotropic glutamate receptor antagonist in animal models of depression. Behav. Brain Res. 2013; 238:48–52. [PubMed: 23098797]
18. Koike H, Iijima M, Chaki S. Involvement of the mammalian target of rapamycin signaling in the antidepressant-like effect of group II metabotropic glutamate receptor antagonists. Neuropharmacology. 2011; 61:1419–1423. [PubMed: 21903115]
19. Karasawa J, Shimazaki T, Kawashima N, Chaki S. AMPA receptor stimulation mediates the antidepressant-like effect of a group II metabotropic glutamate receptor antagonist. Brain Res. 2005; 1042:92–98. [PubMed: 15823257]
20. Ago Y, Yano K, Araki R, Hiramatsu N, Kita Y, Kawasaki T, Onoe H, Chaki S, Nakazato A, Hashimoto H, Baba A, Takuma K, Matsuda T. Metabotropic glutamate 2/3 receptor antagonists improve behavioral and prefrontal dopaminergic alterations in the chronic corticosterone-induced depression model in mice. Neuropharmacology. 2013; 65:29–38. [PubMed: 23022081]
21. Dwyer JM, Lepack AE, Duman RS. mGluR2/3 blockade produces rapid and long-lasting reversal of anhedonia caused by chronic stress exposure. J. Mol. Psychiatry. 2013; 1:15. [PubMed: 25408908]
22. Iijima M, Koike H, Chaki S. Effect of an mGlu2/3 receptor antagonist on depressive behavior induced by withdrawal from chronic treatment with methamphetamine. Behav. Brain Res. 2013; 246:24–28. [PubMed: 23473878]
23. Markou A. Metabotropic glutamate receptor antagonists: Novel therapeutics for nicotine dependence and depression? Biol. Psychiatry. 2007; 61:17–22. [PubMed: 16876138]
24. Ciceroni C, Bonelli M, Mastrantoni E, Niccolini C, Laurenza M, Larocca LM, Pallini R, Traficante A, Spinsanti P, Ricci-Vitiani L, Arcella A, De Maria R, Nicoletti F, Battaglia G, Melchiorri D. Type-3 metabotropic glutamate receptors regulate chemoresistance in glioma stem cells, and their levels are inversely related to survival in patients with malignant gliomas. Cell Death Differ. 2013; 20:396–407. [PubMed: 23175182]
25. Ciceroni C, Arcella A, Mosillo P, Battaglia G, Mastrantoni E, Oliva MA, Carpinelli G, Santoro F, Sale P, Ricci-Vitiani L, De Maria R, Pallini R, Giangaspero F, Nicoletti F, Melchiorri D. Type-3 metabotropic glutamate receptors negatively modulate bone morphogenetic protein receptor signaling and support the tumourigenic potential of glioma-initiating cells. Neuropharmacology. 2008; 55:568–576. [PubMed: 18621067]
26. Arcella A, Carpinelli G, Battaglia G, D'Onofrio M, Santoro F, Ngomba RT, Bruno V, Casolini P, Giangaspero F, Nicoletti F. Pharmacological blockade of group II metabotropic glutamate

receptors reduces the growth of glioma cells in vivo. Neuro-Oncology. 2005; 7:236–245. [PubMed: 16053698]

27. D'Onofrio M, Arcella A, Bruno V, Ngomba RT, Battaglia G, Lombari V, Ragona G, Calogero A, Nicoletti F. Pharmacological blockade of mGlu2/3 metabotropic glutamate receptors reduces cell proliferation in cultured human glioma cells. J. Neurochem. 2003; 84:1288–1295. [PubMed: 12614329]
28. Campo B, Kalinichev M, Lambeng N, Yacoubi ME, Royer-Urios I, Schneider M, Legrand C, Parron D, Girard F, Bessif A, Poli S, Vaugeois J-M, Le Poul E, Celanire S. Characterization of an mGluR2/3 negative allosteric modulator in rodent models of depression. J. Neurogenet. 2011; 25:152–166. [PubMed: 22091727]
29. Pritchett D, Jagannath A, Brown LA, Tam SKE, Hasan S, Gatti S, Harrison PJ, Bannerman DM, Foster RG, Peirson SN. Deletion of metabotropic glutamate receptors 2 and 3 (mGlu2 & mGlu3) in mice disrupts sleep and wheel-running activity, and increases the sensitivity of the circadian system to light. PLoS One. 2015; 10:e0125523. [PubMed: 25950516]
30. Woltering TJ, Wichmann J, Goetschi E, Knoflach F, Ballard TM, Huwyler J, Gatti S. Synthesis and characterization of 1,3-dihydro-benzo[*b*][1,4]diazepin-2-one derivatives: Part 4. In vivo active potent and selective non-competitive metabotropic glutamate receptor 2/3 antagonists. Bioorg. Med. Chem. Lett. 2010; 20:6969–6974. [PubMed: 20971004]
31. Yacoubi, ME.; Vaugeois, J-M.; Kalinichev, M.; Célanire, S.; Parron, D.; Le Poul, E.; Campo, B. Effects of a mGluR2/3 negative allosteric modulator and a reference mGluR2/3 orthosteric antagonist in a genetic mouse model of depression.. Behavioral Studies of Mood Disorders; Proceedings of the 40th Annual Meeting of the Society for Neuroscience; San Diego, CA. Nov 13−17, 2010; Washington, DC: Society for Neuroscience; 2010. 886.14/VV7
32. Goeldner C, Ballard TM, Knoflach F, Wichmann J, Gatti S, Umbricht D. Cognitive impairment in major depression and the mGlu2 receptor as a therapeutic target. Neuropharmacology. 2013; 64:337–346. [PubMed: 22992331]
33. Kalinichev, M.; Campo, B.; Lambeng, N.; Célanire, S.; Schneider, M.; Bessif, A.; Royer-Urios, I.; Parron, D.; Legrand, C.; Mahious, N.; Girard, F.; Le Poul, E. An mGluR2/3 negative allosteric modulator improves recognition memory assessed by natural forgetting in the novel object recognition test in rats.. Memory Consolidation and Reconsolidation: Molecular Mechanisms II; Proceedings of the 40th Annual Meeting of the Society for Neuroscience; San Diego, CA. Nov 13−17, 2010; Washington, DC: Society for Neuroscience; 2010. 406.9/MMM57
34. Choi CH, Schoenfeld BP, Bell AJ, Hinchey P, Kollaros M, Gertner MJ, Woo NH, Tranfaglia MR, Bear MF, Zukin RS, McDonald TV, Jongens TA, McBride SM. Pharmacological reversal of synaptic plasticity deficits in the mouse model of fragile X syndrome by group II mGluR antagonist or lithium treatment. Brain Res. 2011; 1380:106–119. [PubMed: 21078304]
35. Gatti McArthur, S.; Saxe, M.; Wichmann, J.; Woltering, T. mGlu2/3 antagonists for the treatment of autistic disorders.. May 1. 2014 PCT Int. Pat. Appl. WO 2014/064028 A1
36. Structure of decoglurant disclosed in Recommended International Nonproprietary Names (INN). WHO Drug Information. Vol. 27. World Health Organization; Geneva, Switzerland: 2013. p. 150
37. ARTDeCo Study: A study of RO4995819 in patients with major depressive disorder and inadequate response to ongoing antidepressant treatment. U.S. National Institutes of Health; Bethesda, MD: 2011. ClinicalTrials.govhttps://www.clinicaltrials.gov/ct2/show/NCT01457677 (accessed August 12, 2015)
38. Rodriguez AL, Grier MD, Jones CK, Herman EJ, Kane AS, Smith RL, Williams R, Zhou Y, Marlo JE, Days EL, Blatt TN, Jadhav S, Menon UN, Vinson PN, Rook JM, Stauffer SR, Niswender CM, Lindsley CW, Weaver CD, Conn PJ. Discovery of novel allosteric modulators of metabotropic glutamate receptor subtype 5 reveals chemical and functional diversity and in vivo activity in rat behavioral models of anxiolytic and antipsychotic activity. Mol. Pharmacol. 2010; 78:1105–1123. [PubMed: 20923853]
39. Sheffler DJ, Wenthur CJ, Bruner JA, Carrington SJS, Vinson PN, Gogi KK, Blobaum AL, Morrison RD, Vamos M, Cosford NDP, Stauffer SR, Daniels JS, Niswender CM, Conn PJ, Lindsley CW. Development of a novel, CNS-penetrant, metabotropic glutamate receptor 3 ($mGlu_3$) NAM probe (ML289) derived from a closely related $mGlu_5$ PAM. Bioorg. Med. Chem. Lett. 2012; 22:3921–3925. [PubMed: 22607673]

40. Wenthur CJ, Morrison R, Felts AS, Smith KA, Engers JL, Byers FW, Daniels JS, Emmitte KA, Conn PJ, Lindsley CW. Discovery of (*R*)−−(2-fluoro-4-((−4-methoxyphenyl)ethynyl)-phenyl(3-hydroxypiperidin-1-yl)methanone (ML337), An $mGlu_3$ selective and CNS penetrant negative allosteric modulator (NAM). J. Med. Chem. 2013; 56:5208–5212. [PubMed: 23718281]
41. Walker AG, Wenthur CJ, Xiang Z, Rook JM, Emmitte KA, Niswender CM, Lindsley CW, Conn PJ. Metabotropic glutamate receptor 3 activation is required for long-term depression in medial prefrontal cortex and fear extinction. Proc. Natl. Acad. Sci. U. S. A. 2015; 112:1196–1201. [PubMed: 25583490]
42. Zhang L, Balan G, Barreiro G, Boscoe BP, Chenard LK, Cianfrogna J, Claffey MM, Chen L, Coffman KJ, Drozda SE, Dunetz JR, Fonseca KR, Galatsis P, Grimwood S, Lazzaro JT, Mancuso JY, Miller EL, Reese MR, Rogers BN, Sakurada I, Skaddan M, Smith DL, Stepan AF, Trapa P, Tuttle JB, Verhoest PR, Walker DP, Wright AS, Zaleska MM, Zasadny K, Shaffer CL. Discovery and preclinical characterization of 1-methyl-3-(4-methylpyridin-3-yl)-6-(pyridin-2-ylmethoxy)-1*H*-pyrazolo-[3,4-*b*]pyrazine (PF470): a highly potent, selective, and efficacious metabotropic glutamate receptor 5 (mGluR5) negative allosteric modulator. J. Med. Chem. 2014; 57:861–877. [PubMed: 24392688]
43. Zhuo X, Huang XS, Degnan AP, Snyder LB, Yang F, Huang H, Shu Y-Z, Johnson BM. Identification of glutathione conjugates of acetylene-containing positive allosteric modulators of metabotropic glutamate receptor subtype 5. Drug Metab. Dispos. 2015; 43:578–589. [PubMed: 25633841]
44. Noetzel MJ, Rook JM, Vinson PN, Cho H, Days E, Zhou Y, Rodriguez AL, Lavreysen H, Stauffer SR, Niswender CM, Xiang Z, Daniels JS, Jones CK, Lindsley CW, Weaver CD, Conn PJ. Functional impact of allosteric agonist activity of selective positive allosteric modulators of metabotropic glutamate receptor subtype 5 in regulating central nervous system function. Mol. Pharmacol. 2012; 81:120–133. [PubMed: 22021324]
45. Niswender CM, Johnson KA, Luo Q, Ayala JE, Kim C, Conn PJ, Weaver CD. A novel assay of Gi/o-linked G protein-coupled receptor coupling to potassium channels provides new insights into the pharmacology of the group III metabotropic glutamate receptors. Mol. Pharmacol. 2008; 73:1213–1224. [PubMed: 18171729]
46. Conn, PJ.; Lindsley, CW.; Stauffer, SL.; Bartolome-Nebreda, JM.; Conde-Ceide, S.; MacDonald, GJ.; Tong, HM.; Jones, CK.; Alcazar-Vaca, JM.; Andres-Gil, JI.; Malosh, C. Bicyclic triazole and pyrazole lactams as allosteric modulators of mGluR5 receptors.. Jun 21. 2012 PCT Int. Pat. Appl. WO 2012/083224 A1
47. But TYS, Toy PH. The Mitsunobu reaction: Origin, mechanism, improvements, and applications. Chem. - Asian J. 2007; 2:1340–1355. [PubMed: 17890661]
48. Klapars A, Huang X, Buchwald SL. A general and efficient copper catalyst for the amidation of aryl halides. J. Am. Chem. Soc. 2002; 124:7421–7428. [PubMed: 12071751]
49. Gregory KJ, Nguyen ED, Reiff SD, Squire EF, Stauffer SR, Lindsley CW, Meiler J, Conn PJ. Probing the metabotropic glutamate receptor 5 ($mGlu_5$) positive allosteric modulator (PAM) binding pocket: discovery of point mutations that engender a “molecular switch” in PAM pharmacology. Mol. Pharmacol. 2013; 83:991–1006. [PubMed: 23444015]
50. Lamb JP, Engers DW, Niswender CM, Rodriguez AL, Venable DF, Conn PJ, Lindsley CW. Discovery of molecular switches within the ADX-47273 $mGlu_5$ PAM scaffold that modulate modes of pharmacology to afford potent $mGlu_5$ NAMs, PAMs and partial antagonists. Bioorg. Med. Chem. Lett. 2011; 21:2711–2714. [PubMed: 21183344]
51. Kalvass JC, Maurer TS. Influence of nonspecific brain and plasma binding on CNS exposure: implications for rational drug discovery. Biopharm. Drug Dispos. 2002; 23:327–338. [PubMed: 12415573]
52. Bridges TM, Morrison RD, Byers FW, Luo S, Daniels JS. Use of a novel rapid and resource-efficient cassette dosing approach to determine the pharmacokinetics and CNS distribution of small molecule 7-transmembrane receptor allosteric modulators in rat. Pharmacol. Res. Perspect. 2014; 2:e00077. [PubMed: 25505618]
53. Leeson PD, Springthorpe B. The influence of drug-like concepts on decision-making in medicinal chemistry. Nat. Rev. Drug Discovery. 2007; 6:881–890. [PubMed: 17971784]

54. Obach RS. Prediction of human clearance of twenty-nine drugs from hepatic microsomal intrinsic clearance data: An examination of in vitro half-life approach and nonspecific binding to microsomes. Drug Metab. Dispos. 1999; 27:1350–1359. [PubMed: 10534321]

55. Davies B, Morris T. Physiological parameters in laboratory animals and humans. Pharm. Res. 1993; 10:1093–1095. [PubMed: 8378254]

56. Bridges TM, Rook JM, Noetzel MJ, Morrison RD, Zhou Y, Gogliotti RD, Vinson PN, Xiang Z, Jones CK, Niswender CM, Lindsley CW, Stauffer SL, Conn PJ, Daniels JS. Biotransformation of a novel positive allosteric modulator of metabotropic glutamate receptor subtype 5 contributes to seizure-like adverse events in rats involving a receptor agonism-dependent mechanism. Drug Metab. Dispos. 2013; 41:1703–1714. [PubMed: 23821185]

57. Di L, Rong H, Feng B. Demystifying brain penetration in central nervous system drug discovery. J. Med. Chem. 2013; 56:2–12. [PubMed: 23075026]

58. Hemstapat K, Da Costa H, Nong Y, Brady AE, Luo Q, Niswender CM, Tamagnan GD, Conn PJ. A novel family of potent negative allosteric modulators of group II metabotropic glutamate receptors. J. Pharmacol. Exp. Ther. 2007; 322:254–264. [PubMed: 17416742]

59. LeadProfilingScreen; (catalogue no. 68). Eurofins Panlabs, Inc.; Redmond, WA: (www.eurofinspanlabs.com)

60.

Significant responses are defined as those that inhibited more than 50% of radioligand binding.

61. Fitzgerald LW, Burn TC, Brown BS, Patterson JP, Corjay MH, Valentine PA, Sun JH, Link JR, Abbaszade I, Hollis JM, Largent BL, Hartig PR, Hollis GF, Meunier PC, Robichaud AJ, Robertson DW. Possible role of valvular serotonin 5-HT(2B) receptors in the cardiopathy associated with fenfluramine. Mol. Pharmacol. 2000; 57:75–81. [PubMed: 10617681]

62. *Serotonin (5-Hydroxytryptamine) 5-HT2B, IP1*; (catalogue no. 355260). Eurofins Panlabs, Inc.; Redmond, WA: (www.eurofinspanlabs.com)

63. Zientek M, Miller H, Smith D, Dunklee MB, Heinle L, Thurston A, Lee C, Hyland R, Fahmi O, Burdette D. Development of an in vitro drug-drug interaction assay to simultaneously monitor five cytochrome P450 isoforms and performance assessment using drug library compounds. J. Pharmacol. Toxicol. Methods. 2008; 58:206–214. [PubMed: 18634893]

64. Wang Q, Rager JD, Weinstein K, Kardos PS, Dobson GL, Li J, Hidalgo IJ. Evaluation of the MDR-MDCK cell line as a permeability screen for the blood−brain barrier. Int. J. Pharm. 2005; 288:349–359. [PubMed: 15620875]

65. Njung'e K, Handley SL. Evaluation of marble-burying behavior as a model of anxiety. Pharmacol., Biochem. Behav. 1991; 38:63–67. [PubMed: 2017455]

66. Njung'e K, Handley SL. Effects of 5-HT uptake inhibitors, agonists and antagonists on the burying of harmless objects by mice; a putative test for anxiolytic agents. Br. J. Pharmacol. 1991; 104:105–112. [PubMed: 1686200]

67. Nicolas LB, Kolb Y, Prinssen EP. A combined marble burying-locomotor activity test in mice: a practical screening test with sensitivity to different classes of anxiolytics and antidepressants. Eur. J. Pharmacol. 2006; 547:106–115. [PubMed: 16934246]

68. Felts AS, Rodriguez AL, Morrison RD, Venable DF, Manka JT, Bates BS, Blobaum AL, Byers FW, Daniels JS, Niswender CM, Jones CK, Conn PJ, Lindsley CW, Emmitte KA. Discovery of VU0409106: A negative allosteric modulator of mGlu5 with activity in a mouse model of anxiety. Bioorg. Med. Chem. Lett. 2013; 23:5779–5785. [PubMed: 24074843]

69. Thomas A, Burant A, Bui N, Graham D, Yuva-Paylor LA, Paylor R. Marble burying reflects a repetitive and perseverative behavior more than novelty-induced anxiety. Psychopharmacology. 2009; 204:361–373. [PubMed: 19189082]

70. Cosford ND, Tehrani L, Roppe J, Schweiger E, Smith ND, Anderson J, Bristow L, Brodkin J, Jiang X, McDonald I, Rao S, Washburn M, Varney MA. 3-[(2-Methyl-1,3-thiazol-4-yl)-ethynyl]-pyridine: a potent and highly selective metabotropic glutamate subtype 5 receptor antagonist with anxiolytic activity. J. Med. Chem. 2003; 46:204–206. [PubMed: 12519057]

71. Detke MJ, Rickels M, Lucki I. Active behaviors in the rat forced swimming test differentially produced by serotonergic and noradrenergic antidepressants. Psychopharmacology (Berl). 1995; 121:66–72. [PubMed: 8539342]

72. Garcia LS, Comim CM, Valvassori SS, Réus GZ, Barbosa LM, Andreazza AC, Stertz L, Fries GR, Gavioli EC, Kapczinski F, Quevedo J. Acute administration of ketamine induces antidepressant-like effects in the forced swimming test and increases BDNF levels in the rat hippocampus. Prog. Neuro-Psychopharmacol. Biol. Psychiatry. 2008; 32:140–144.
73. Kohrs R, Durieux ME. Ketamine: Teaching an old drug new tricks. Anesth. Analg. 1998; 87:1186–1193. [PubMed: 9806706]
74. Murrough JW, Iosifescu DV, Chang LC, Al Jurdi RK, Green CE, Perez AM, Iqbal S, Pillemer S, Foulkes A, Shah A, Charney DS, Mathew SJ. Antidepressant efficacy of ketamine in treatment-resistant major depression: a two-site randomized controlled trial. Am. J. Psychiatry. 2013; 170:1134–1142. [PubMed: 23982301]
75. Browne CA, Lucki I. Antidepressant effects of ketamine: mechanisms underlying fast-acting novel antidepressants. Front. Pharmacol. 2013; 4 DOI: 10.3389/fphar.2013.00161.
76. aan het Rot M, Collins KA, Murrough JW, Perez AM, Reich DL, Charney DS, Mathew SJ. Safety and efficacy of repeated-dose intravenous ketamine for treatment-resistant depression. Biol. Psychiatry. 2010; 67:139–145. [PubMed: 19897179]
77. Morgan CJA, Curran HV. Ketamine use: A review. Addiction. 2012; 107:27–38. [PubMed: 21777321]
78. Zhou W, Wang N, Yang C, Li X-M, Zhou Z-Q, Yang J-J. Ketamine-induced antidepressant effects are associated with AMPA receptors-mediated upregulation of mTOR and BDNF in rat hippocampus and prefrontal cortex. Eur. Psychiatry. 2014; 29:419–423. [PubMed: 24321772]
79. Koike H, Chaki S. Requirement of AMPA receptor stimulation for the sustained antidepressant activity of ketamine and LY341495 during the forced swim test in rats. Behav. Brain Res. 2014; 271:111–115. [PubMed: 24909673]
80. Duman RS, Li N, Liu R-J, Duric V, Aghajanian G. Signaling pathways underlying the rapid antidepressant actions of ketamine. Neuropharmacology. 2012; 62:35–41. [PubMed: 21907221]
81. Dwyer JM, Lepack AE, Duman RS. mTOR activation is required for the antidepressant effects of $mGluR_{2/3}$ blockade. Int. J. Neuropsychopharmacol. 2012; 15:429–434. [PubMed: 22114864]
82. Li N, Lee B, Liu RJ, Banasr M, Dwyer JM, Iwata M, Li XY, Aghajanian G, Duman RS. mTOR-dependent synapse formation underlies the rapid antidepressant effects of NMDA antagonists. Science. 2010; 329:959–964. [PubMed: 20724638]

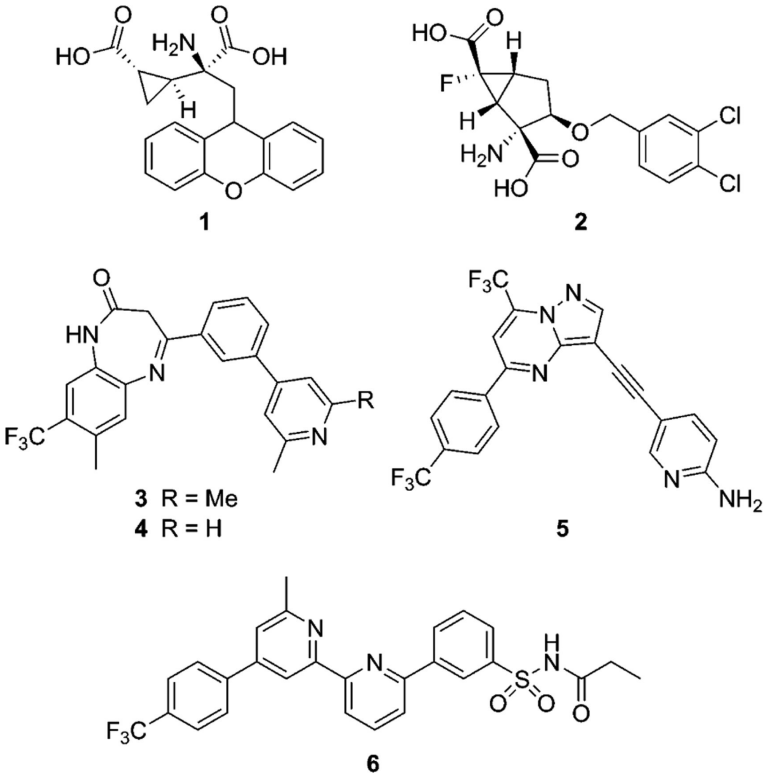

Figure 1.

$mGlu_{2/3}$ orthosteric antagonist tools **1** and **2**, $mGlu_{2/3}$ NAM tools **3, 4,** and **6**, and Roche $mGlu_{2/3}$ NAM clinical compound **5**.

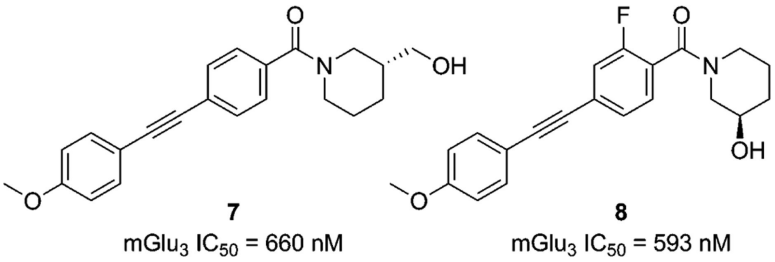

Figure 2.

$mGlu_3$ NAMs from the 1,2-diphenylethyne chemotype.

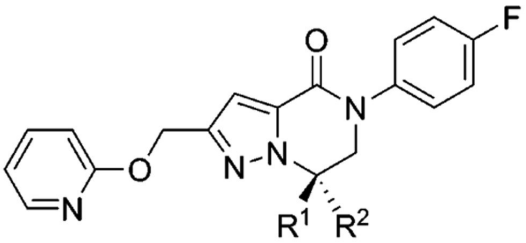

9	$R^1 = R^2 = H$	$mGlu_3$ IC_{50} = 569 nM (NAM) $mGlu_5$ EC_{50} = 140 nM (PAM)
10	$R^1 = Me, R^2 = H$	$mGlu_3$ IC_{50} = 401 nM (NAM) $mGlu_5$ EC_{50} = 276 nM (PAM)
11	$R^1 = H, R^2 = Me$	$mGlu_3$ IC_{50} > 10 μM (weak NAM) $mGlu_5$ EC_{50} = 212 nM (PAM)

Figure 3.
Representative compounds from a new $mGlu_3$ lead series.

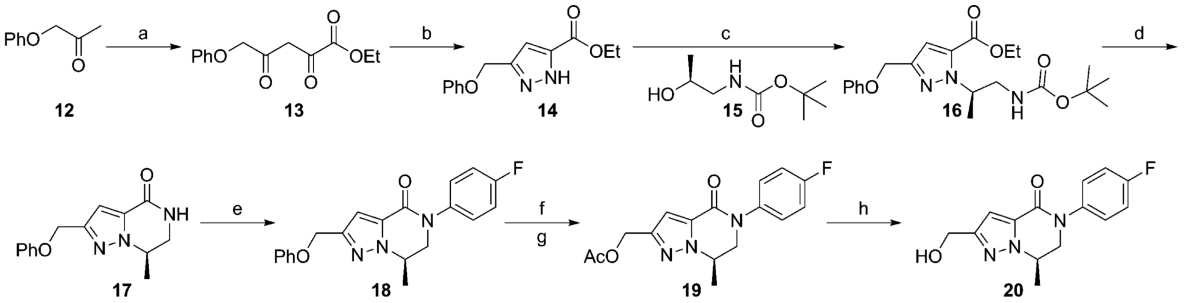

[a]Reagents and conditions: (a) Na, EtOH, $(EtO_2C)_2$, 0 °C to rt, 27%; (b) $NH_2NH_2{\cdot}H_2O$, EtOH, 80 °C, 98%; (c) PPh_3, D^{t}BAD, THF, μwave, 120 °C, 20 min; (d) 4 M HCl in dioxane, then saturated aq $NaHCO_3$, 74%, 2 steps; (e) CuI, K_2CO_3, 4-fluorobromobenzene, *N,N′*-dimethylethylenediamine, PhMe, 120 °C, 83%; (f) BBr_3, CH_2Cl_2, 0 °C to rt; (g) KOAc, DMF, 60 °C, 100%, 2 steps; (h) 1 M aq LiOH, MeOH, THF, 94%.

Scheme 1.

Synthesis of Primary Alcohol Intermediate 20[a]

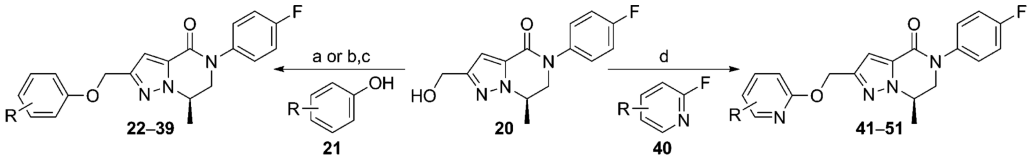

[a]Reagents and conditions: (a) PS-PPh$_3$, THF, DIAD, 7−37%; (b) NEt$_3$, MsCl, CH$_2$Cl$_2$, 63%; (c) Cs$_2$CO$_3$, DMF, 90 °C, 35−52%; (d) NaH, DMF, 8−37%.

Scheme 2.

Synthesis of New Western Ether Analogues 22–39 and 41–51[a]

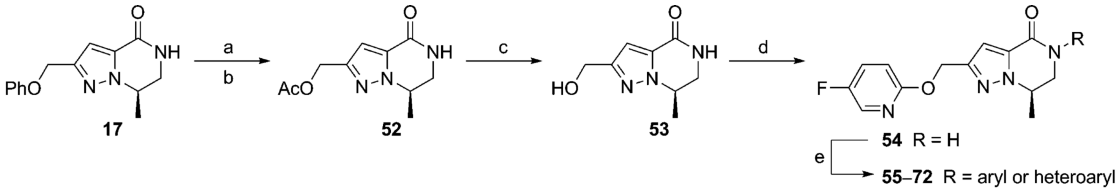

[a]Reagents and conditions: (a) BBr_3, CH_2Cl_2, 0 °C to rt; (b) KOAc, DMF, 60 °C, 54%, 2 steps; (c) 1 M aq LiOH, MeOH, THF, 37%; (d) NaH, DMF, 2,5-difluoropyridine, 76%; (e) CuI, K_2CO_3, aryl or heteroaryl halide, *N,N′*-dimethylethylenediamine, PhMe, 120 °C, 17–70%.

Scheme 3.

Synthesis of 5-Fluoropyridin-2-yl Ether Analogues 55–72[a]

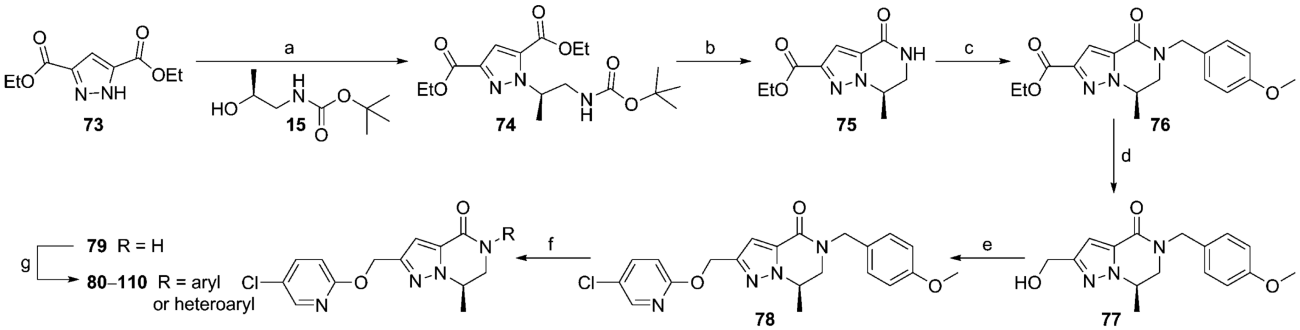

[a]Reagents and conditions: (a) PPh_3, D[t]BAD, THF, μwave, 120 °C, 20 min; (b) 4 M HCl in dioxane, then saturated aq $NaHCO_3$, 89%, 2 steps; (c) NaH, 4-methoxybenzyl chloride, DMF, 0 °C to rt, 73%; (d) $NaBH_4$, THF, MeOH, 0–60 °C, 84%; (e) NaH, DMF, 5-chloro-2-fluoropyridine, 0 °C to rt, 84%; (f) $(NH_4)_2Ce(NO_3)_6$, MeCN, H_2O, 66%; (g) CuI, K_2CO_3, aryl or heteroaryl halide, *N*,*N*′-dimethylethylenediamine, PhMe, 120 °C,16–99%.

Scheme 4.

Synthesis of 5-Chloropyridin-2-yl Ether Analogues 80–110[a]

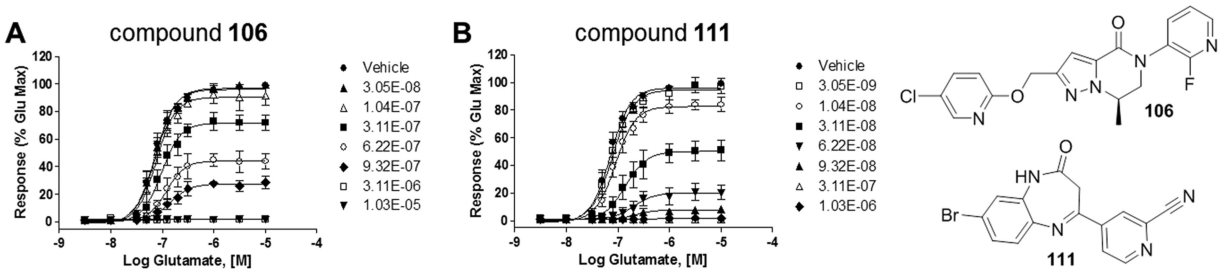

Figure 4.

Progressive fold-shift of the glutamate CRC by $mGlu_3$ NAM **106** (A) and $mGlu_{2/3}$ NAM **111** (B); compound concentrations shown in M.

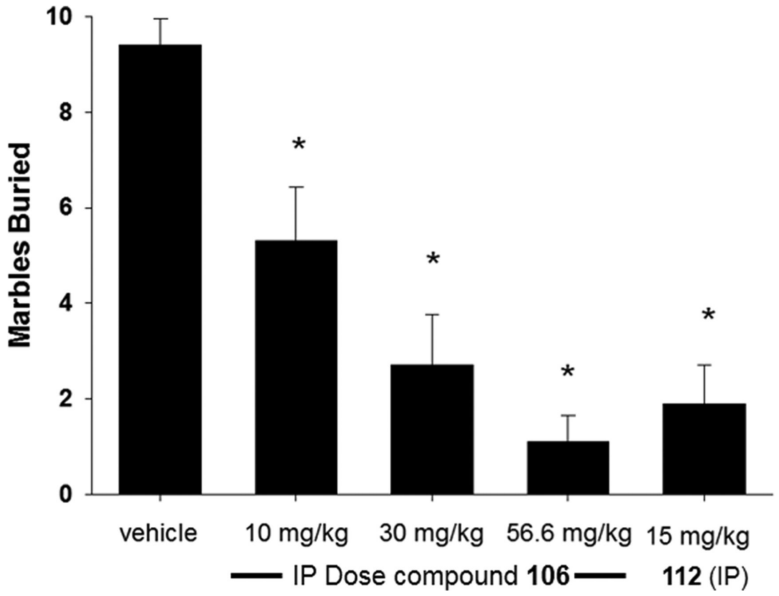

Figure 5.

Inhibition of marble burying in mice by compound **106**. *n* = 8–10 male CD-1 mice per treatment group; vehicle = 10% Tween 80 in H_2O; 15 min pretreatment with compound or vehicle; 30 min burying time; *, $p < 0.05$ vs vehicle control group. Compound **112** is the $mGlu_5$ NAM 3-[(2-methyl-1,3-thiazol-4-yl)ethynyl]-pyridine.

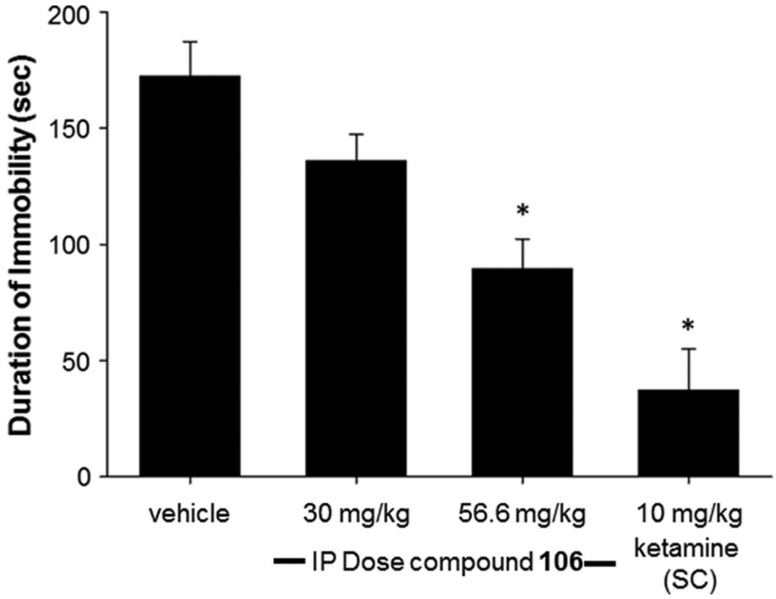

Figure 6.

Decrease in immobility in the FST in rats by compound **106**. *n* = 8–10 male Sprague–Dawley rats per treatment group; **106** vehicle = 10% Tween 80 in H_2O; ketamine vehicle = saline; 30 min pretreatment with compound or vehicle; 6 min testing session; *, $p < 0.05$ vs vehicle control group.

Table 1

$mGlu_3$ NAM and $mGlu_5$ SAR of Western Phenyl Ethers 18, 22–39

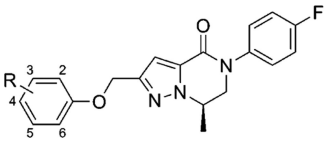

no.	R	$mGlu_3$ pIC_{50} (± SEM)[a]	$mGlu_3$ IC_{50} (nM)[a]	% Glu Max (± SEM)[a,b]	$mGlu_5$ activity[c]	$mGlu_5$ pEC_{50} (± SEM)[c]	$mGlu_5$ EC_{50} (nM)[c]	% Glu Max (± SEM)[b,c]
18	H	6.57 ± 0.15	267	2.21 ± 0.80	PAM	7.34 ± 0.02	46	87.7 ± 1.4
22	2-F	6.28 ± 0.20	530	2.90 ± 1.05	PAM	6.71 ± 0.04	195	89.3 ± 3.0
23	3-F	6.11 ± 0.03	773	1.19 ± 0.75	PAM	7.14 ± 0.02	73	86.1 ± 2.9
24	4-F	6.34 ± 0.04	462	2.09 ± 0.57	PAM	7.03 ± 0.05	92	87.0 ± 1.0
25	2,4-di-F	6.38 ± 0.22	417	1.70 ± 0.35	PAM	6.51 ± 0.05	307	82.3 ± 2.7
26	2-Me	6.14 ± 0.14	721	1.56 ± 0.37	PAM	5.83 ± 0.04	1500	83.7 ± 2.5
27	3-Me	5.84 ± 0.05	1440	2.35 ± 0.18	NAM[d]	<5.0	>10000	39.7 ± 7.7
28	4-Me	5.92 ± 0.02	1190	1.72 ± 0.55	PAM	5.97 ± 0.04	1080	92.5 ± 2.6
29	2-Cl	6.27 ± 0.18	532	1.63 ± 0.33	PAM	6.38 ± 0.01	419	84.4 ± 2.1
30	3-Cl	5.79 ± 0.02	1620	1.96 ± 0.11	NAM[d]	<5.0	>10000	32.8 ± 6.1
31	4-Cl	5.93 ± 0.01	1170	1.86 ± 0.52	PAM	6.22 ± 0.04	604	81.8 ± 0.3
32	2-OMe	5.59 ± 0.18	2540	2.32 ± 1.39	PAM[d]	<5.0	>10000	63.7 ± 3.1
33	3-OMe	5.89 ± 0.02	1290	1.78 ± 0.53	PAM	5.74 ± 0.04	1840	32.4 ± 3.0
34	4-OMe	5.98 ± 0.02	1040	1.76 ± 0.39	PAM	5.87 ± 0.16	1340	40.2 ± 4.8
35	4-CF_3	5.73 ± 0.01	1850	4.13 ± 0.09		<4.5	>30000	
36	4-Et	6.08 ± 0.05	830	2.29 ± 0.84	PAM	5.49 ± 0.03	3210	50.8 ± 3.7
37	4-CN	6.11 ± 0.12	784	2.53 ± 0.70	PAM	5.71 ± 0.06	1940	38.6 ± 4.8
38	4-OEt	5.94 ± 0.06	1160	3.39 ± 0.87		<4.5	>30000	
39	4-OCF_3	5.39 ± 0.04	4070	2.66 ± 0.34		<4.5	>30000	

[a] Calcium mobilization mGlu3 assay; values are average of $n \geq 3$.

[b] Amplitude of response in the presence of 30 μM test compound as a percentage of maximal response (100 μM glutamate); average of $n \geq 3$.

[c] Calcium mobilization mGlu5 assay; values are average of $n \geq 3$.

[d] Weak activity; concentration response curve (CRC) does not plateau.

Table 2

$mGlu_3$ NAM and $mGlu_5$ SAR of Western 2-Pyridyl Ethers 41–51

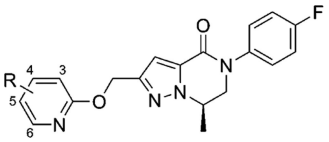

no.	R	$mGlu_3$ pIC_{50} (± SEM)[a]	$mGlu_3$ IC_{50} (nM)[a]	% Glu Max (± SEM)[a,b]	$mGlu_5$ activity[c]	$mGlu_5$ pEC_{50} (± SEM)[c]	$mGlu_5$ EC_{50} (nM)[c]	% Glu Max (± SEM)[b,c]
41	3-F	5.96 ± 0.02	1100	2.22 ± 0.84	PAM	5.37 ± 0.06	4300	78.5 ± 6.1
42	3-CF_3	5.53 ± 0.02	2940	2.11 ± 0.96		<4.5	>30000	
43	3-OMe	5.17 ± 0.02	6760	–1.14 ± 2.54		<4.5	>30000	
44	4-Me	5.68 ± 0.01	2090	0.86 ± 0.47	NAM[d]	<5.0	>10000	46.9 ± 5.9
45	4-CF_3	5.78 ± 0.01	1670	1.62 ± 0.42	NAM[d]	<5.0	>10000	12.9 ± 2.9
46	4-OMe	5.43 ± 0.00	3690	–0.18 ± 1.39	NAM[d]	<5.0	>10000	54.7 ± 5.8
47	5-F	6.27 ± 0.02	539	1.71 ± 0.55	NAM[d]	<5.0	>10000	46.5 ± 3.4
48	5-Cl	6.22 ± 0.04	605	1.84 ± 0.51	PAM	5.53 ± 0.06	2920	81.4 ± 2.7
49	6-Me	5.62 ± 0.02	2370	1.12 ± 1.08	NAM	5.65 ± 0.07	2250	2.47 ± 0.17
50	6-CF_3	5.63 ± 0.02	2360	2.06 ± 0.79		<4.5	>30000	
51	6-OMe	5.80 ± 0.02	1590	1.94 ± 0.62	PAM[d]	<5.0	>10000	31.2 ± 3.1

[a] Calcium mobilization mGlu3 assay; values are average of $n \geq 3$.

[b] Amplitude of response in the presence of 30 μM test compound as a percentage of maximal response (100 μM glutamate); average of $n \geq 3$.

[c] Calcium mobilization mGlu5 assay; values are average of $n \geq 3$.

[d] Weak activity; CRC does not plateau.

Table 3

DMPK Profiling of Early Analogues

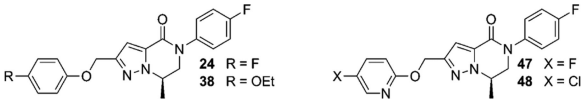

no.	cLogP[a]	LLE[b]	$mGlu_3$ IC_{50} (nM)	fold vs $mGlu_5$	rat plasma F_u[c]		CL_{plasma} (mL/min/kg)[d]	V_{SS} (L/kg)[d]
24	3.96	2.38	462	0.20	0.060	95	40	3.5
38	4.24	1.70	1160	>25	0.005	32	82	2.2
47	3.06	3.21	539	>18	0.135	88	82	6.6
48	3.57	2.65	605	4.8	0.034	141	29	5.2

[a]Calculated using Dotmatics Elemental (www.dotmatics.com/products/elemental/).

[b]LLE (ligand-lipophilicity efficiency) = pIC_{50} – cLogP.

[c]F_u = fraction unbound.

[d]Rat IV PK results (n = 2); dose = 0.2 mg/kg; solution in 9% EtOH, 37% PEG 400, 54% DMSO (2 mg/mL).

Table 4

mGlu$_3$ NAM and mGlu$_5$ SAR of 5-Fluoropyridin-2-yl Ether Analogues 55–72

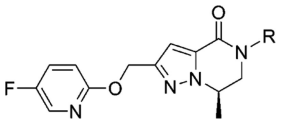

no.	R	mGlu$_3$ pIC$_{50}$ (± SEM)[a]	mGlu$_3$ IC$_{50}$ (nM)[a]	% Glu Max (± SEM)[a,b]	mGlu$_5$ activity[c]	mGlu$_5$ pEC$_{50}$ (± SEM)[c]	mGlu$_5$ EC$_{50}$ (nM)[c]	% Glu Max (± SEM)[b,c]
55	2-fluorophenyl	6.79 ± 0.17	162	1.53 ± 0.12	NAM[f]	<5.0	>10000	29.1 ± 7.3
56	3-fluorophenyl	6.72 ± 0.08	192	1.44 ± 0.38	NAM	5.56 ± 0.24	2720	9.71 ± 5.78
57	2-chlorophenyl	6.85 ± 0.16	141	1.37 ± 0.72	NAM	6.00 ± 0.25	1010	8.78 ± 5.29
58	3-chlorophenyl	6.84 ± 0.10	145	2.30 ± 0.17	NAM[e]	5.73 ± 0.24	1850	19.2 ± 10.0
59	4-chlorophenyl	6.71 ± 0.13	197	2.17 ± 0.40	PAM	6.44 ± 0.03	364	51.6 ± 7.7
60	2-methylphenyl	6.46 ± 0.06	346	1.72 ± 0.16	NAM[f]	<5.0[d]	>10000[d]	35.8[d]
61	3-methylphenyl	6.67 ± 0.15	216	1.93 ± 0.56	NAM[f]	<5.0	>10000	36.6 ± 8.7
62	4-methylphenyl	6.57 ± 0.03	269	1.04 ± 0.45	NAM[f]	<5.0	>10000	54.8 ± 9.4
63	2-methoxyphenyl	6.47 ± 0.10	339	1.49 ± 0.60	NAM	6.52 ± 0.17	301	3.28 ± 0.45
64	3-methoxyphenyl	6.70 ± 0.06	198	1.02 ± 0.12	NAM[f]	<5.0	>10000	59.7 ± 6.1
65	4-methoxyphenyl	6.49 ± 0.10	320	1.23 ± 0.38	PAM	5.86 ± 0.05	1380	32.3 ± 5.2
66	2,3-difluorophenyl	6.73 ± 0.16	184	2.15 ± 0.33	NAM[e]	5.68 ± 0.20	2110	21.0 ± 10.6
67	2,5-difluorophenyl	6.91 ± 0.11	123	2.62 ± 0.47	NAM[f]	<5.0	>10000	18.8 ± 6.1
68	2,6-difluorophenyl	6.74 ± 0.08	181	1.49 ± 0.17	NAM[e]	5.91[d]	1230[d]	50.8[d]
69	pyridin-2-yl	6.04 ± 0.05	915	0.96 ± 0.63	NAM	5.45 ± 0.04	3520	3.71 ± 0.47
70	pyridin-3-yl	6.36 ± 0.13	436	0.64 ± 0.70	NAM[f]	<5.0	>10000	46.3 ± 2.9
71	pyridin-4-yl	6.05 ± 0.04	881	0.77 ± 0.44		<4.5	>30000	
72	5-fluoropyridin-2-yl	6.46 ± 0.07	349	1.31 ± 0.11	NAM	5.01 ± 0.13	9740	7.0 ± 2.5

[a] Calcium mobilization mGlu3 assay; values are average of $n \geq 3$.

[b] Amplitude of response in the presence of 30 μM test compound as a percentage of maximal response (100 μM glutamate); average of $n \geq 3$.

[c] Calcium mobilization mGlu5 assay; values are average of $n \geq 3$.

[d] Average of $n = 2$.

[e] Partial NAM; CRC plateaus above 10% glutamate maximum.

[f] Weak activity; CRC does not plateau.

Table 5

In Vitro DMPK Profiling of Select 5-Fluoropyridin-2-yl Ether Analogues

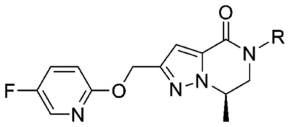

no.	R	cLogP[a]	LLE[b]	$mGlu_3$ IC_{50} (nM)	fold vs $mGlu_5$	rat plasma F_u[c]	rat CL_{hep} (mL/min/kg)[d]
55	2-fluorophenyl	3.06	3.73	162	>61	0.098	64.7
56	3-fluorophenyl	3.06	3.66	192	14	0.094	53.0
57	2-chlorophenyl	3.57	3.28	141	7.2	0.054	66.5
58	3-chlorophenyl	3.57	3.27	145	13	0.034	51.9
61	3-methylphenyl	3.23	3.44	216	17	0.051	58.4
66	2,3-difluorophenyl	3.16	3.57	184	11	0.092	63.6
67	2,5-difluorophenyl	3.16	3.75	123	>81	0.089	49.6
68	2,6-difluorophenyl	3.16	3.58	181	6.8	0.064	64.6

[a] Calculated using Dotmatics Elemental (www.dotmatics.com/products/elemental/).

[b] LLE (ligand-lipophilicity efficiency) = pIC_{50} – cLogP.

[c] F_u = fraction unbound.

[d] Predicted hepatic clearance based on intrinsic clearance in rat liver microsomes.

Table 6

mGlu$_3$ NAM and mGlu$_5$ SAR of 5-Chloropyridin-2-yl Ether Analogues 80–101

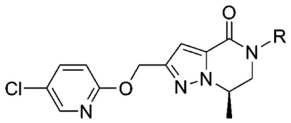

no.	R	mGlu$_3$ pIC$_{50}$ (± SEM)[a]	mGlu$_3$ IC$_{50}$ (nM)[a]	% Glu Max (± SEM)[a,b]	mGlu$_5$ activity[c]	mGlu$_5$ pEC$_{50}$ (± SEM)[c]	mGlu$_5$ EC$_{50}$ (nM)[c]	% Glu Max (± SEM)[b,c]
80	2-fluorophenyl	6.65 ± 0.04	226	1.74 ± 0.10	PAM	5.49 ± 0.06	3240	57.3 ± 4.6
81	3-fluorophenyl	6.69 ± 0.04	206	1.38 ± 0.47	PAM	5.22 ± 0.05	5970	63.5 ± 0.8
82	2-chlorophenyl	6.48 ± 0.08	328	1.87 ± 0.29	PAM	5.26 ± 0.03	5450	51.0 ± 3.9
83	3-chlorophenyl	6.25 ± 0.07	558	1.63 ± 0.20	PAM	5.54 ± 0.02	2870	65.8 ± 8.8
84	4-chlorophenyl	5.91 ± 0.25	1230	0.94 ± 1.46	PAM	5.48 ± 0.15	3310	51.2 ± 10.3
85	2-methylphenyl	6.24 ± 0.18	571	1.95 ± 0.70	PAM	5.64 ± 0.03	2280	80.7 ± 0.5
86	3-methylphenyl	6.41 ± 0.05	392	1.71 ± 0.44	PAM	5.44 ± 0.11	3600	69.9 ± 6.5
87	4-methylphenyl	6.39 ± 0.21	410	1.39 ± 0.25	PAM[e]	<5.0	>10000	70.8 ± 3.1
88	2-methoxyphenyl	6.16 ± 0.15	690	1.29 ± 0.18	NAM[e]	<5.0	>10000	58.5 ± 1.2
89	3-methoxyphenyl	6.50 ± 0.05	313	2.00 ± 0.32	PAM	5.29 ± 0.08	5070	78.0 ± 1.8
90	4-methoxyphenyl	6.36 ± 0.11	439	2.07 ± 0.68	PAM	5.36 ± 0.06	4330	59.4 ± 7.3
91	2-cyanophenyl	6.37 ± 0.05	429	1.64 ± 0.04	PAM	5.30 ± 0.10	4970	38.1 ± 5.0
92	3-cyanophenyl	6.08 ± 0.26	825	1.75 ± 0.41	PAM[e]	<5.0	>10000	32.2 ± 3.7
93	4-cyanophenyl	6.27 ± 0.05	539	1.84 ± 0.19	PAM	5.48 ± 0.08	3320	23.1 ± 6.8
94	2,3-difluorophenyl	6.07 ± 0.23	852	0.33 ± 0.71	PAM	5.17 ± 0.29	6680	36.1 ± 8.4
95	2,4-difluorophenyl	6.55 ± 0.08	280	1.34 ± 0.25	PAM	5.59 ± 0.07	2580	70.8 ± 0.8
96	2,6-difluorophenyl	6.65 ± 0.04	225	2.06 ± 0.31	PAM	5.85 ± 0.09	1420	40.3 ± 5.6
97	3,5-difluorophenyl	6.38 ± 0.07	420	2.18 ± 0.19	PAM[e]	<5.0	>10000	33.1 ± 2.3
98	2-cyano-5-fluorophenyl	6.28 ± 0.06	529	1.55 ± 0.31		<4.5	>30000	
99	3-cyano-5-fluorophenyl	6.50 ± 0.07	315	1.92 ± 0.12	PAM	5.98[d]	1044[d]	28.0[d]
100	pyridin-2-yl	6.48 ± 0.07	328	1.07 ± 0.04		<4.5	>30000	
101	pyridin-3-yl	6.22 ± 0.10	608	1.73 ± 0.53		<4.5	>30000	

[a] Calcium mobilization mGlu3 assay; values are average of $n \geq 3$.

[b] Amplitude of response in the presence of 30 μM test compound as a percentage of maximal response (100 μM glutamate); average of $n \geq 3$.

[c] Calcium mobilization mGlu5 assay; values are average of $n \geq 3$.

[d] Average of $n = 2$.

[e] Weak activity; CRC does not plateau.

Table 7

$mGlu_3$ NAM and $mGlu_5$ SAR of Additional 5-Chloropyridin-2-yl Ether Analogues 102–110

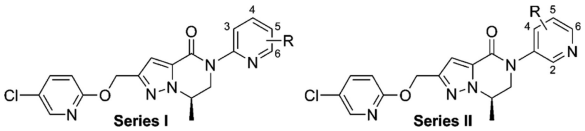

no.	series	R	$mGlu_3$ pIC_{50} (± SEM)[a]	$mGlu_3$ IC_{50} (nM)[a]	% Glu Max (± SEM)[a,b]	$mGlu_5$ activity[c]	$mGlu_5$ pEC_{50} (± SEM)[c]	$mGlu_5$ EC_{50} (nM)[c]	% Glu Max (± SEM)[b,c]
102	I	3-F	6.44 ± 0.03	362	1.64 ± 0.36	PAM[d]	<5.0	>10000	32.4 ± 4.4
103	I	3-CN	6.17 ± 0.06	677	1.35 ± 0.55		<4.5	>30000	
104	I	5-F	6.59 ± 0.09	260	2.44 ± 0.32	PAM[d]	<5.0	>10000	47.9 ± 5.1
105	I	6-F	6.53 ± 0.08	294	1.75 ± 0.19	NAM[d]	<5.0	>10000	24.8 ± 5.5
106	II	2-F	6.41 ± 0.05	392	1.71 ± 0.41		<4.5	>30000	
107	II	4-F	6.32 ± 0.03	482	1.45 ± 0.22		<4.5	>30000	
108	II	5-F	6.32 ± 0.03	481	1.85 ± 0.32		<4.5	>30000	
109	II	5-CN	6.22 ± 0.01	605	1.08 ± 0.50		<4.5	>30000	
110	II	6-F	6.39 ± 0.06	408	1.45 ± 0.29	PAM[d]	<5.0	>10000	30.6 ± 2.4

[a] Calcium mobilization $mGlu_3$ assay; values are average of $n \geq 3$.

[b] Amplitude of response in the presence of 30 μM test compound as a percentage of maximal response (100 μM glutamate); average of $n \geq 3$.

[c] Calcium mobilization $mGlu_5$ assay; values are average of $n \geq 3$.

[d] Weak activity; CRC does not plateau.

Table 8

In Vitro DMPK Profiling of Select 5-Chloropyridin-2-yl Ether Analogues

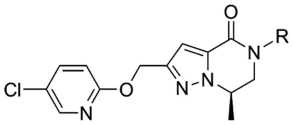

no.	R	cLogP[a]	LLE[b]	$mGlu_3$ IC_{50} (nM)	fold vs $mGlu_5$	rat plasma F_u[c]	rat CL_{hep} (mL/min/kg)[d]
99	2-cyano-5-fluorophenyl	3.29	2.99	529	>56	0.045	47.7
100	pyridin-2-yl	2.57	3.91	328	>91	0.051	69.5
101	pyridin-3-yl	2.16	4.06	608	>49	0.118	42.0
106	2-fluoropyridin-3-yl	2.67	3.74	392	>76	0.083	36.9
107	4-fluoropyridin-3-yl	2.26	4.06	482	>62	0.085	36.0
108	5-fluoropyridin-3-yl	2.26	4.06	481	>62	0.092	26.6
109	5-cyanopyridin-3-yl	1.88	4.34	605	>49	0.078	22.8

[a]Calculated using Dotmatics Elemental (www.dotmatics.com/products/elemental/).

[b]LLE (ligand-lipophilicity efficiency) = pIC_{50} – cLogP.

[c]F_u = fraction unbound.

[d]Predicted hepatic clearance based on intrinsic clearance in rat liver microsomes.

Table 9

In Vivo DMPK Profiling of Select 5-Chloropyridin-2-yl Ether Analogues

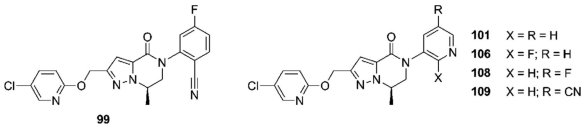

			rat IV PK results[b]			rat IP tissue distribution results[c,d,e]			
no.	**rat plasma F_u[a]**	**rat brain F_u[a]**	**$t_{1/2}$ (min)**	**CL_{plasma} (mL/min/kg)**	**V_{SS} (L/kg)**	**plasma conc (μM)**	**brain conc (μM)**	**K_p[f]**	**$K_{p,uu}$[g]**
99	0.045	0.032	194	13	2.2	1.68	2.41	1.4	1.0
101	0.118		21	50	1.2				
106	0.083	0.052	42	37	1.6	9.49	15.85	1.7	1.0
108	0.092		30	50	1.9				
109	0.078	0.033	59	22	1.4	4.52	5.28	1.2	0.49

[a] F_u = fraction unbound.

[b] n = 2; dose = 0.2 mg/kg; solution in 10% EtOH, 38–40% PEG 400, 50–52% DMSO (2 mg/mL).

[c] n = 2; time point = 15 min; dose = 10 mg/kg.

[d] For **99** and **109**, fine homogeneous suspension in 0.1% Tween 80 and 0.5% methyl cellulose in H_2O (4 mg/mL).

[e] For **106**, fine homogeneous suspension in 10% EtOH and 90% PEG400 (4 mg/mL).

[f] K_p = total brain to total plasma ratio.

[g] $K_{p,uu}$ = unbound brain (brain F_u × total brain) to unbound plasma (plasma F_u × total plasma) ratio

Table 10

P450 Inhibition and Permeability Profile of Compound 106

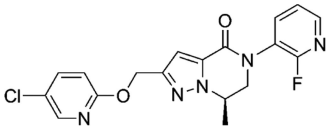

P450 inhibition[a]		permeability[b]	
CYP1A2 IC_{50}	>30 μM	A–B P_{app}	45.0×10^{-6} cm/s
CYP2C9 IC_{50}	25.6 μM	B–A P_{app}	49.9×10^{-6} cm/s
CYP2D6 IC_{50}	>30 μM	efflux ratio	1.1
CYP3A4 IC_{50}	>30 μM		

[a]Cocktail assay in HLM.

[b]MDR1-MDCK cells.

Table 11

Rodent PK Profile of Compound 106

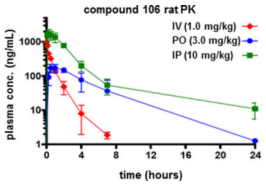

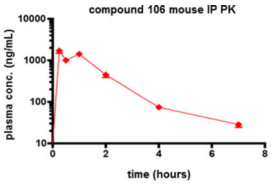

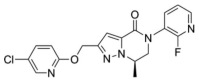

Protein Binding (F_u)[a]		Rat IP PK[b]	
rat plasma	0.083	dose	10 mg/kg
rat brain homogenates	0.052	plasma C_{max}	4.57 ± 0.67 μM
mouse plasma	0.163	plasma T_{max}	12.3 ± 2.7 minutes
mouse brain homogenates	0.035	plasma $AUC_{0-\infty}$	11.5 ± 0.4 μM·h

Rat IV[c] and PO[d] PK		Mouse IP Tissue Distribution[e]				Mouse IP PK[h]	
$t_{1/2}$	49 minutes	dose		10 mg/kg		dose	10 mg/kg
CL_{plasma}	30 mL/min/kg	plasma concentration		2.59 ± 0.29 μM		plasma C_{max}	4.48 ± 0.56 μM
V_{SS}	1.4 L/kg	brain concentration		9.36 ± 0.61 μM		plasma T_{max}	30 ± 15 minutes
F	60%	K_p[f]	$K_{p,uu}$[g]	3.6	0.78	plasma $AUC_{0-\infty}$	7.26 ± 0.24 μM·h

[a] F_u = fraction unbound.

[b] n = 3; fine microsuspension in 0.1% Tween 80 and 0.5% methyl cellulose in H_2O (4 mg/mL).

[c] n = 2; dose =1.0 mg/kg; solution in 10% EtOH, 50% PEG 400, 40% saline (1 mg/mL).

[d] n = 2; dose = 3.0 mg/kg; fine microsuspension in 0.1% Tween 80 and 0.5% methyl cellulose in H_2O (0.3 mg/mL).

[e] n = 3; time point = 30 min post dose; fine microsuspension in 0.1% Tween 80 and 0.5% methyl cellulose in H_2O (1 mg/mL).

[f] K_p = total brain to total plasma ratio.

[g] $K_{p,uu}$ = unbound brain (brain F_u × total brain) to unbound plasma (plasma F_u × total plasma) ratio.

[h] n = 3 per time point; fine microsuspension in 0.1% Tween 80 and 0.5% methyl cellulose in H_2O (1 mg/mL).